Molecular Plant
Research Article

CellPress
PARTNER JOURNAL

The High Light Response and Redox Control of Thylakoid FtsH Protease in *Chlamydomonas reinhardtii*

Fei Wang, Yafei Qi, Alizée Malnoë, Yves Choquet, Francis-André Wollman and Catherine de Vitry*

Institut de Biologie Physico-Chimique, Unité Mixte de Recherche 7141, Centre National de la Recherche Scientifique/Université Pierre et Marie Curie, Paris 75005, France

***Correspondence: Catherine de Vitry (catherine.devitry@ibpc.fr)**

http://dx.doi.org/10.1016/j.molp.2016.09.012

ABSTRACT

In *Chlamydomonas reinhardtii*, the major protease involved in the maintenance of photosynthetic machinery in thylakoid membranes, the FtsH protease, mostly forms large hetero-oligomers (~1 MDa) comprising FtsH1 and FtsH2 subunits, whatever the light intensity for growth. Upon high light exposure, the FtsH subunits display a shorter half-life, which is counterbalanced by an increase in *FTSH1/2* mRNA levels, resulting in the modest upregulation of FtsH1/2 proteins. Furthermore, we found that high light increases the protease activity through a hitherto unnoticed redox-controlled reduction of intermolecular disulfide bridges. We isolated a *Chlamydomonas FTSH1* promoter-deficient mutant, *ftsh1-3*, resulting from the insertion of a *TOC1* transposon, in which the high light-induced upregulation of *FTSH1* gene expression is largely lost. In *ftsh1-3*, the abundance of FtsH1 and FtsH2 proteins are loosely coupled (decreased by 70% and 30%, respectively) with no formation of large and stable homo-oligomers. Using strains exhibiting different accumulation levels of the FtsH1 subunit after complementation of *ftsh1-3*, we demonstrate that high light tolerance is tightly correlated with the abundance of the FtsH protease. Thus, the response of *Chlamydomonas* to light stress involves higher levels of FtsH1/2 subunits associated into large complexes with increased proteolytic activity.

Key words: chloroplast protease, regulation of gene expression, photoinhibition, *Chlamydomonas reinhardtii*

Wang F., Qi Y., Malnoë A., Choquet Y., Wollman F.-A., and de Vitry C. (2017). The High Light Response and Redox Control of Thylakoid FtsH Protease in *Chlamydomonas reinhardtii*. Mol. Plant. **10**, 99–114.

INTRODUCTION

The unicellular green alga *Chlamydomonas reinhardtii*, a photosynthetic model organism, attracts increasing attention for its ability to evolve hydrogen and to accumulate reduced carbon in lipids and starch (reviewed by Grossman et al., 2011; Merchant et al., 2012). As land plants, *Chlamydomonas* requires light energy to drive electron flow from photosystem II (PSII) to photosystem I (PSI) and then to NADPH, while generating the proton gradient required to synthesize ATP, both of which are subsequently used for carbon fixation. However, excess light is harmful to photosynthetic organisms. Indeed, it leads to the over-reduction of the electron transport chain and generates reactive oxygen species (ROS), for instance singlet oxygen ($^1O_2$) in PSII (Szilárd et al., 2005) or superoxide (O_2^-) in PSI (Krieger-Liszkay et al., 2011), which cause oxidative damages to chloroplast DNA, lipids, and proteins, consequently decreasing biomass productivity (Burgess et al., 2015; Kerchev et al., 2015; Murchie et al., 2015). *Chlamydomonas* has developed responses aimed at preventing or repairing high light (HL)-induced damage (reviewed by Erickson et al., 2015). A well-characterized response is the PSII repair cycle, conserved from cyanobacteria to vascular plants (reviewed by Nixon et al., 2010; Komenda et al., 2012; Järvi et al., 2015). This cycle involves the migration of photodamaged PSII complexes to thylakoid margins, their partial disassembly, the degradation of damaged D1 subunit by the cooperative action of Deg and FtsH proteases, and its replacement by a newly synthesized D1 polypeptide (Lindahl et al., 2000; Kapri-Pardes et al., 2007; Sun et al., 2007; Kato et al., 2012).

FtsH is an ATP-dependent zinc metalloprotease, ubiquitous in prokaryotes and chloroplasts and mitochondria of eukaryotes (Akiyama et al., 1995; reviewed by Janska et al., 2013). While FtsH is encoded by a unique gene in most prokaryotes, multiple isoforms are found in cyanobacteria, algae, and plants.

Published by the Molecular Plant Shanghai Editorial Office in association with Cell Press, an imprint of Elsevier Inc., on behalf of CSPB and IPPE, SIBS, CAS.

In *Arabidopsis*, at least four members of the FtsH family, FtsH1/5 (type A) and FtsH2/8 (type B), are localized in the thylakoid membrane where they form a heterohexameric ring structure resembling its prokaryotic counterparts (Krzywda et al., 2002; Niwa et al., 2002; Yu et al., 2004, 2005; Zaltsman et al., 2005b). Mutations in FtsH5 and two respectively confer the *var1* and *var2* variegated phenotype to leaves, which become sensitive to photoinhibition (Chen et al., 2000; Sakamoto et al., 2002). In the thylakoid of *Chlamydomonas*, two FtsH isoforms only, FtsH1 (type A) and FtsH2 (type B), form the hetero-oligomers that are required for D1 degradation (Malnoë et al., 2014). The *ftsh1-1* mutant expressing an inactive FtsH1 protein is highly sensitive to HL stress (Malnoë et al., 2014). FtsH regulation by HL remains largely unexplored in *Chlamydomonas* apart from the findings that *FTSH1/2* mRNA levels increase upon HL (Duanmu et al., 2013) and FtsH1/2 proteins increase upon oxidative stress (Barth et al., 2014).

FtsH also plays a major role in the turnover of the cytochrome b_6f complex, being responsible for its active degradation in nitrogen-starved cells (Wei et al., 2014) or when misassembled because of lacking some hemes (Malnoë et al., 2011, 2014). Mutants lacking any CCB factor (cofactor assembly on cytochrome b_6f complex subunit PetB), required for the covalent binding of heme c_i to cytochrome b_6 (Kuras et al., 2007), cannot grow phototrophically and show a strongly reduced accumulation of cytochrome b_6f subunits (Kuras et al., 1997; de Vitry et al., 2004). Two suppressor mutations, which restore both phototrophy and the accumulation of the cytochrome b_6f complex subunits, have been isolated from *ccb* mutants. These mutations, *ftsh1-1* and *ftsh1-2*, both lead to the substitution of a conserved critical residue (R420C and T382I, respectively) that inactivates the FtsH1 protein while preserving wild-type (WT) protein accumulation level. Here, we characterized suppressor mutation *ftsh1-3*, which is affected in the promoter region of the gene and thus lacks most of the FtsH1 protein. We used complemented strains to assess the correlation between the abundance of the FtsH protease and the tolerance to HL stress. We analyzed the *in vivo* regulation of the FtsH protease at the transcript and protein levels (including protein lifetime and oligomerization) in response to HL. We provide experimental evidence for a post-translational regulation of FtsH activity in response to HL via a redox control of FtsH disulfide bridges.

RESULTS

FtsH1 and FtsH2 Are Both Induced under High Light

FTSH transcripts are upregulated by HL in *Arabidopsis* and *Chlamydomonas* (Sinvany-Villalobo et al., 2004; Duanmu et al., 2013). To further understand the light response of *FTSH1/2* expression in *Chlamydomonas*, we transferred WT cells grown to mid-log phase under low light (LL) to HL. The accumulation of *FTSH1/2* transcripts and protein products was then monitored at different time points. In real-time quantitative PCR (qPCR) analysis, *GBLP*, encoding a guanine nucleotide-binding protein subunit β-like protein, was used as a reference gene (Schloss, 1990; Maruyama et al., 2014) and *GSTS1*, encoding glutathione *S*-transferase, as a positive control for HL induction (Fischer et al., 2006). Upon transfer to HL, *GSTS1* transcript accumulation was, as expected, increased by up to nine-fold after 1 h (Fischer et al., 2012). The accumulation of *FTSH1* transcripts also rose rapidly, about 3.5-fold after 15 min, and reached a peak (approximately seven-fold) after 30 min, before returning to a stationary level, three- to four-fold higher than in LL conditions (Figure 1A). *FTSH2* shows similar induction kinetics (Figure 1A), suggesting that it shares a common induction pathway with *FTSH1*.

At the protein level, the accumulation of FtsH1/2 increased steadily during 4 h of HL, up to 1.6-fold compared with their level under LL (Figure 1B, see also a summary of transcript and protein accumulation levels in different strains and conditions in Supplemental Table 1). The much lower increase in protein accumulation, when compared with the transcriptional induction, could be due to a further regulation step at the level of translation or to an increased turnover of FtsH under HL. To assess FtsH turnover we added an inhibitor of cytosolic translation, cycloheximide, to the cell culture when transferred under HL. As expected, the inhibition of *de novo* synthesis of FtsH prevented its induction under HL (Figure 1C). In addition, while FtsH1/2 were stable for at least 4 h under LL, they both showed a marked decrease under HL, with a half-life of about 2 h (Figure 1C). A general effect of cycloheximide under HL stress leading to massive proteolysis of thylakoid proteins is excluded by the overall unaltered protein content on a chlorophyll basis. Thus, the increased turnover of FtsH under HL is consistent with the limited increase in FtsH proteins under HL despite a seven-fold increase in transcript abundance.

Given that the accumulation of *FTSH* transcripts accompanies with the ROS-induced increase in *GSTS1* transcript (Fischer et al., 2005), we looked at whether reactive nitrogen species (RNS) production elicited *FTSH* upregulation. Nitric oxide (NO) is produced by *Chlamydomonas* cells under very HL (Chang et al., 2013) or during nitrogen starvation concomitantly with the FtsH-mediated degradation of cytochrome b_6f subunits (Wei et al., 2014). We therefore tested the response of *FTSH1* and *FTSH2* gene expression to variations of NO levels. While the level of *GSTS1* transcript indeed increased upon addition of an NO inducer and decreased in the presence of an NO scavenger, those of *FTSH1* and *FTSH2* remained insensitive to the same additions in all conditions tested, therefore not supporting an NO-mediated stimulation of *FTSH* gene expression (Supplemental Figure 1).

Isolation of an FtsH Promoter Mutant, $Su_{4\text{-}ccb4}$, Showing Low Accumulation of FtsH1 and Slightly Reduced Level of FtsH2

In an attempt to further understand the dynamics of *FTSH* expression changes with light intensity, we looked for mutated strains that would express lower amounts of the FtsH under various light regimes. To this end, we searched for phenotypic suppressors of *ccb* mutations (Malnoë et al., 2014) that would express lower amounts of the FtsH protease. The non-phototrophic *ccb4-1* mutant bears a mutation generating a stop codon in *CCB4* gene, and therefore is deficient in the CCB4 factor required for covalent binding of heme c_i to cytochrome b_6 and shows a strongly reduced accumulation of cytochrome b_6f subunits (Kuras et al., 2007). We recovered a spontaneous

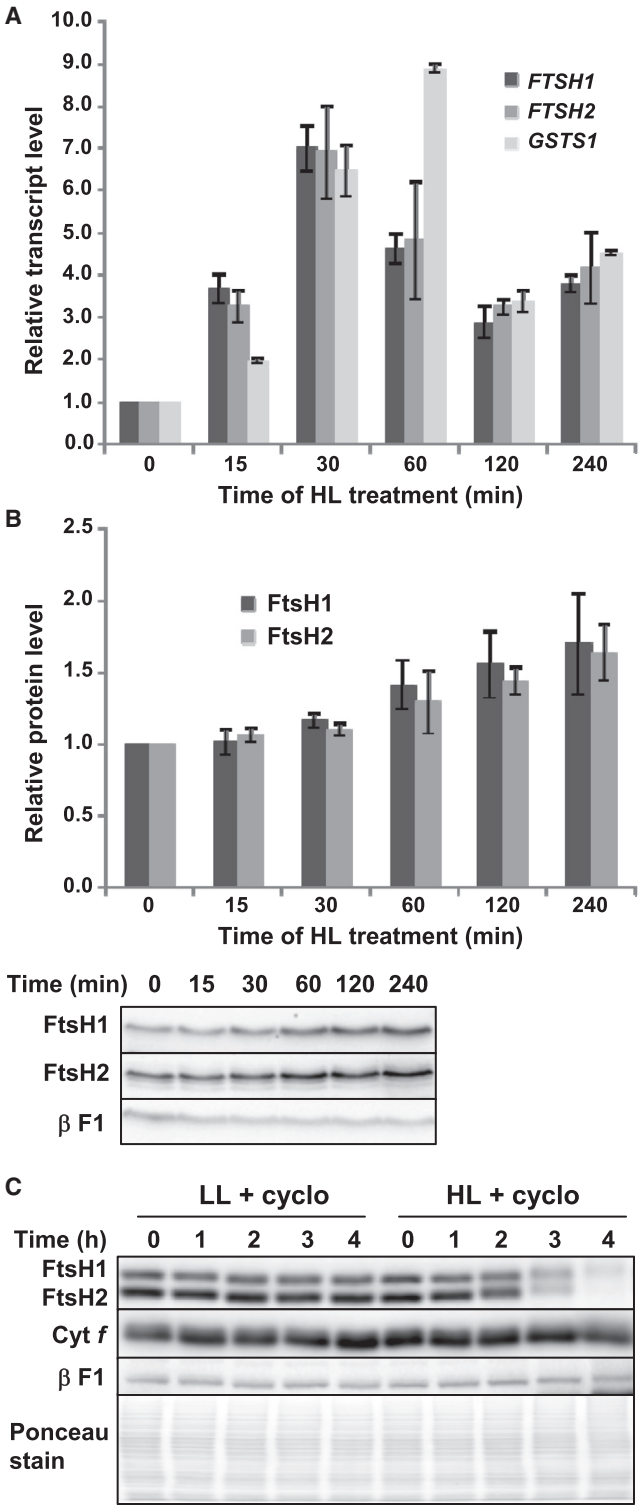

Figure 1. The Expression of *FTSH* Genes Is Upregulated upon High Light Illumination.

(A) Transcript levels for *FTSH1/2* genes determined in WT cells by real-time qPCR at the indicated time points following transfer to high light (HL; 1000 μmol photons m^{-2} s^{-1}), after normalization to the reference gene *GBLP*. The HL-regulated nuclear gene *GSTS1* was used as a positive control. Data represent means ± SD of six independent experiments.

(B) Accumulation of FtsH1 and FtsH2 proteins in samples from **(A)**, assessed by immunoblots (one representative immunoblot is shown below the graph). Whole-cell protein extracts loaded on a chlorophyll basis were separated by 8% SDS–PAGE in the presence of 8 M urea and immunodetected with antibodies against FtsH1/2 or against the β-subunit of mitochondrial ATP synthase (β F1) as a loading control. Accumulation of FtsH subunits was normalized to that of the loading control, β F1. Data represent means ± SD of three independent experiments.

(C) Lifetime of FtsH subunits in WT cells exposed to low light (LL; 10 μmol photons m^{-2} s^{-1}) or HL (1000 μmol photons m^{-2} s^{-1}), determined by immunochase experiment. Cycloheximide (30 μg ml^{-1}), an inhibitor of cytosolic translation, was added to an exponentially growing culture of cells under LL, just before the transfer of half culture to HL. The FtsH1 and FtsH2 accumulation was immunodetected in samples harvested at the indicated time points. Cytochrome *f*, β F1, and Ponceau red-stained membrane show the overall unaltered protein content on a chlorophyll basis.

phenotypic revertant, *Rccb4-SR1*, which restored a limited photosynthetic growth capability (Figure 2A) and a WT accumulation of cytochrome b_6f subunits (Figure 2B) without heme c_i binding to cytochrome b_6, as assessed by peroxidase activity staining (Figure 2B, lower panel). This result is consistent with the lack of CCB4 and the lower accumulation of CCB2, two homologous proteins required for the covalent binding of heme c_i to the apocytochrome b_6 subunit (Kuras et al., 2007; Saint-Marcoux et al., 2009). By crossing the *Rccb4-SR1* strain with the WT strain WT S24$^-$ (CC-5100), we isolated the suppressor mutation, $Su_{4\text{-}ccb4}$, in a WT background for *CCB4*. We then monitored the expression of the *FTSH* genes in this mutant. RNA blot showed an approximately five-fold reduced accumulation of *FTSH1* transcripts, but unaltered accumulation of *FTSH2* transcripts (Figure 3A). Immunoblots showed that FtsH1 accumulation was heavily compromised in strains *Rccb4-SR1* and $Su_{4\text{-}ccb4}$, being reduced by more than 70%, while FtsH2 still accumulated to about 70% of its WT content (Figure 3B). Accordingly, $Su_{4\text{-}ccb4}$ showed higher sensitivity to photoinhibition than the WT strain (Supplemental Figure 2).

The mutation causing the decreased *FTSH1* expression in strain $Su_{4\text{-}ccb4}$ could affect the *FTSH1* locus itself or any other loci controlling its expression, such as that encoding the G protein α-subunit GPA1, required for FtsH expression in *Arabidopsis* (Zhang et al., 2009). In a cross with the interfertile and polymorphic strain S1-D2 (CC-2290, Rymarquis et al., 2005), the mutant phenotype segregated 2:2 and cosegregated with the *FTSH1* AFLP marker typical of the *C. reinhardtii* parent (see Methods and Supplemental Figure 3). This indicated a single nuclear mutation, tightly linked to the *FTSH1* gene that was identified by sequencing the genome of *Rccb4-SR1* (together with that of the isogenic *ccb4* parental strain for comparison). After alignment of the reads along the reference genome, a complete *TOC1* transposon (Day et al., 1988; Day and Rochaix, 1991) was found upstream of the *FTSH1* CDS, in reverse orientation compared with *FTSH1* (Supplemental Figures 4 and 5).

The annotation of the *FTSH1* mRNA in the Phytozome V10.5 database suggests a 5′ untranslated region (UTR) of 348 nt. However, EST sequences found in NCBI and transcriptomic data available at http://genomes.mcdb.ucla.edu/Cre454 support a shorter 5′ UTR of 104 nt. To determine the actual 5′ UTR end, we designed primers within or upstream of the short 5′ UTR. Supplemental Figure 4B shows that only the shorter

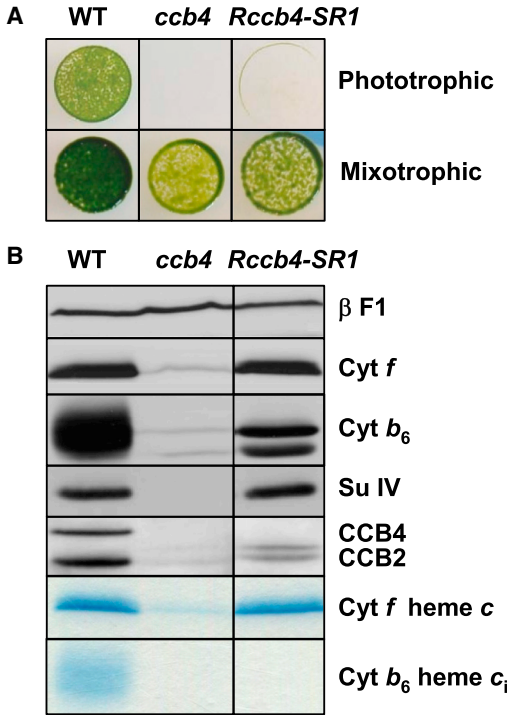

Figure 2. Revertant *Rccb4-SR1* Recovered Some Phototrophic Growth Capability and Wild-Type Level of Cytochrome b_6f Complexes.

(A) Phototrophic growth of wild-type (WT), *ccb4* mutant, and *Rccb4-SR1* revertant on minimal medium plates and mixotrophic growth on acetate-containing TAP medium, shown for comparison, after 7 days of growth under 30 μmol photons m^{-2} s^{-1} illumination.

(B) Whole-cell protein extracts from the same strains grown mixotrophically (6 μmol photons m^{-2} s^{-1}) were separated by SDS–PAGE on a 12%–18% polyacrylamide gel in the presence of 8 M urea and immunodetected with antibodies against cytochrome b_6f subunits (cytochrome *f*, cytochrome b_6, and subunit IV), CCB factors (CCB2 and CCB4), and against β F1 as a loading control. As previously observed (Saint-Marcoux et al., 2009; Malnoë et al., 2014), CCB2 accumulates as a doublet in the absence of CCB4. Heme peroxidase activity carried by heme *c* of cytochrome *f* and heme c_i of cytochrome b_6 was detected by tetramethylbenzamidine staining (Thomas et al., 1976). Same experiment as in Malnoë et al. (2014) (showing *Rccb4-301* but not *Rccb4-SR1*) with WT and *ccb4* provided as control lanes now for *Rccb4-SR1* (not showing *Rccb4-301*).

5′ UTR could be amplified from cDNA in 5′-RACE (rapid amplification of cDNA ends) experiments, in agreement with the transcriptomic data. *TOC1* is inserted 120 nt upstream of the AUG start codon, which thus lie in the promoter region of *FTSH1*, 16 bp upstream of transcript 5′ end. To confirm that this *TOC1* insertion was responsible for the $Su_{4\text{-}ccb4}$ phenotype, we transformed this latter strain with the pSL18-g*FTSH1* plasmid carrying both the paromomycin resistance gene *APHVII* and the *gFTSH1* gene driven by the *PSAD* 5′ UTR and promoter regions (Malnoë et al., 2014; Figure 4A). Transformed clones, selected for paromomycin resistance, showed restored FtsH1 accumulation (Figure 4B) and increased HL tolerance (Figure 4C). Thus, *TOC1*, inserted in the *FTSH1* promoter, knocks down FtsH1 expression in $Su_{4\text{-}ccb4}$, thereby suppressing the phototrophic defect in the *ccb4* mutant. Consequently, we renamed the $Su_{4\text{-}ccb4}$ mutation *ftsh1-3*.

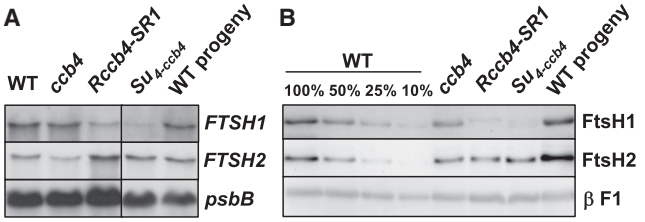

Figure 3. The $Su_{4\text{-}ccb4}$ Suppressor Mutation Leads to Reduced Expression of the *FTSH1* Gene.

(A) Accumulation of *FTSH1* and *FTSH2* transcripts detected by hybridization with specific DNA probes in the *ccb4* mutant, in the *Rccb4-SR1* revertant, and in two progeny from the cross *Rccb4-SR1* × WT, one ($Su_{4\text{-}ccb4}$) carrying only the suppressor mutation in a WT *CCB4* background, while the other (WT progeny) carries WT alleles for both $Su_{4\text{-}ccb4}$ and *CCB4* loci. *psbB* transcript provides a loading control.

(B) Accumulation of FtsH1 and FtsH2 proteins in whole-cell protein extracts from the same strains. A dilution series of the WT is shown for comparison, and β F1 provides a loading control.

Disruption of the *FTSH1* Promoter Compromises High Light-induced Upregulation of *FTSH1*

The mutant *ftsh1-3* harbors a truncated *FTSH1* promoter and may lack transcriptional *cis*-regulatory elements. We then assessed its HL responsiveness. To this end, we replaced the *PSAD* promoter in our transformation vector by either the very short region of the *FTSH1* promoter left after the insertion of *TOC1* (pSP construct) or a longer fragment containing 500 bp upstream of the initiation codon (pLP construct), as shown in Figure 5A. Transformants, selected for paromomycin resistance, were then screened by PCR for insertion of the full-length SP/LP-*gFTSH1* constructs. We selected 11 (out of 43) and 14 (out of 44) clones, respectively showing the correct insertion of the pLP and pSP constructs, for further analysis by chlorophyll fluorescence (Supplemental Figure 6A) and immunoblot assay of FtsH1 accumulation (Supplemental Figure 6B): on average, LP transformants were less affected by HL and accumulated higher levels of FtsH1 than SP transformants or strain *ftsh1-3*.

The HL response was further analyzed in transformants *S35* and *L19*. Based on the results shown in Figure 1, time points of 30 min were chosen for real-time qPCR analysis and 30 min and 2 h for protein quantification. Induction ratio, calculated as the amount of transcripts under HL over that under LL, amounted to 8 in WT, but remained around 3 in strains *ftsh1-3*, *S35*, and *L19* (Figure 5B). The transcriptional induction of *FTSH2* was similar in WT and in the three mutant strains, thus independent of that of *FTSH1* (Figure 5B). Real-time qPCR data were further confirmed by dot blots (Figure 5B). That we still observed an induction in *FTSH1* transcription upon HL in both the *ftsh1-3* and *S35* strains indicates that critical HL-responsive elements were retained with the shorter version of the *FTSH1* promoter region. However, that light induction remained much lower than in the WT, even with the longer promoter construct we used in L19, suggests that there are still HL-responsive *cis*-regulatory elements upstream of the region conserved in the LP construct. Indeed, the new PLACE software (https://sogo.dna.affrc.go.jp/cgi-bin/sogo.cgi?sid=&lang=en&pj=640& action=page& page=newplace; Higo et al., 1999) predicts several

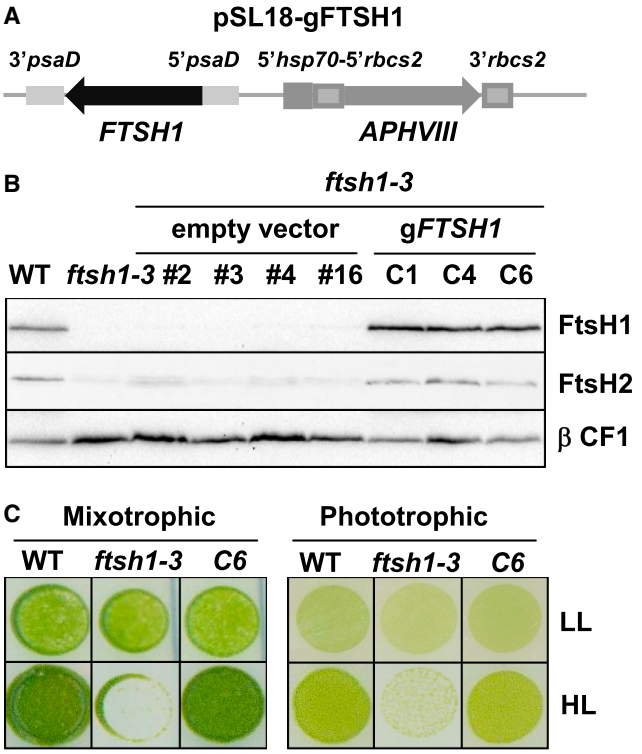

Figure 4. Complementation of the *ftsh1-3* Mutation by a *PSAD*-Driven *FTSH1* Gene.

(A) Schematic map of the pSL18-g*FTSH1* plasmid used for complementation. Genomic DNA encompassing the *FTSH1* CDS is inserted between the *PSAD* 5′ and 3′ UTRs. The adjacent *APHVIII* cassette allows selection of transformants on paromomycin-supplemented plates.

(B) Accumulation of FtsH1 and FtsH2 proteins in clones transformed by the empty vector pSL18 or by the pSL18-g*FTSH1* plasmid. β CF1 provides a loading control.

(C) Phototrophic (minimal medium) and mixotrophic (TAP) growth of the *ftsh1-3* mutant and of a representative complemented strain grown for 5 days under LL (10 μmol photons m^{-2} s^{-1}) or HL (100 μmol photons m^{-2} s^{-1}). WT is shown for comparison.

potential light-responsive elements, such as SORLIP 1, SORLIP 2, and G-BOX (Hudson and Quail, 2003; Park et al., 2013) in the promoter regions of *FTSH1* and *FTSH2*, most of them upstream of the region retained in the LP construct (Supplemental Figure 7). Loss of some of these potential regulatory elements in the *ftsh1-3* or *S35* may also explain the decrease of *FTSH1* transcripts under LL. The accumulation of the FtsH1 protein in all the tested strains after 2 h of HL (Figure 5C) was consistent with RNA levels, being modestly induced by 1.3-fold (Supplemental Table 1) while the accumulation of FtsH2 was induced to the same extent as in WT (Figure 5C).

Expression Levels of FtsH1 Contribute to Controlling Tolerance to High Light

That defective FtsH protease leads to increased photosensitivity is well established, but the precise correlation between the accumulation of FtsH and the HL tolerance has not yet been addressed. As the WT, *ftsh1-3*, *S35*, or *L19* strains displayed contrasting amounts of FtsH, we monitored the maximum quantum efficiency of PSII primary photochemistry by calculating the F_v/F_m ratio from fluorescence induction kinetics (Baker, 2008) in these strains, exposed for 1 h to HL and allowed to recover for 3 h in LL. F_v/F_m dropped quickly during the first 10 min of HL (Figure 6), at a time when the FtsH protein is not yet induced (Figure 1B). The most rapid drop in F_v/F_m was observed in *ftsh1-3* compared with that in *S35* and *L19*, whereas the slowest was observed in WT. Similarly, the recovery of F_v/F_m was the best in WT and the most limited in *ftsh1-3*. Thus, the abundance of FtsH1 in the various strains correlates with the tolerance to photoinhibition (Figure 6A) as well as with the growth capability under HL, either on Tris-acetate-phosphate (TAP) or minimal medium (Figure 6B).

Most transformants recovered upon complementation of the *ftsh1-3* mutant with the pSL18–g*FTSH1* construct accumulated a higher level of FtsH1 than the WT (Figure 4B). One of them, *C6*, was selected to further test the effect of FtsH1 overexpression on photoinhibition. Under LL, the *FTSH1* transcript accumulated three times more in strain *C6* than in WT (Figure 7A), resulting in a 1.3-fold increased protein accumulation (Figure 7B). However, since transcription of *FTSH1* is not induced by HL when driven by the exogenous *PSAD* promoter, the abundance of FtsH1 protein was similar in WT and *C6* strains after 2 h of HL. When tested for PSII activity after 1 h of HL, the higher accumulation of FtsH in *C6* seems to confer a little more tolerance to photoinhibition (F_v/F_m 0.35) than the WT (F_v/F_m 0.25) but this difference in PSII activity was lost upon recovery under LL (Figure 7C, left panel). To test the role of FtsH induction, we added cycloheximide to WT and *C6* cultures when shifted from LL to HL. As expected, the inhibition of *de novo* synthesis of FtsH prevented part of the recovery but preserved a significantly higher PSII activity in *C6* than in WT upon recovery (Figure 7C, right panel). We also monitored the accumulation of D1 fragments in the above conditions. The accumulation of D1 fragments was negatively correlated with the recovery from photoinhibition, cycloheximide-treated WT after 1 h of HL having the lowest amount of FtsH and the higher accumulation of D1 fragments (Supplemental Figure 8A). As expected, HL treatment for twice as long showed increased photoinhibition and larger differences between *C6* and WT (Supplemental Figure 8B). Together, these experiments demonstrate that both the initial amount of FtsH and its induction upon HL are critical for the resistance to HL stress in *Chlamydomonas*.

FtsH1 and FtsH2 Show a Concerted Accumulation in Large Complexes

Numerous studies have shown the oligomeric nature of the FtsH protease (for reviews, see Langklotz et al., 2012; Janska et al., 2013). In *Thermus thermophilus* and *Escherichia coli*, FtsH forms a homohexameric ring structure (Krzywda et al., 2002; Niwa et al., 2002). By contrast, heterohexamers are found in the thylakoids of photosynthetic organisms such as cyanobacteria (Boehm et al., 2012), *Arabidopsis* (Yu et al., 2005; Zaltsman et al., 2005b), and *Chlamydomonas* (Malnoë et al., 2014). The increased expression of *FTSH* genes in HL that is accompanied by a shortening of the half-life of the two *FTSH* gene products suggests possible post-translational changes that may affect the oligomeric state of FtsH. In addition, the

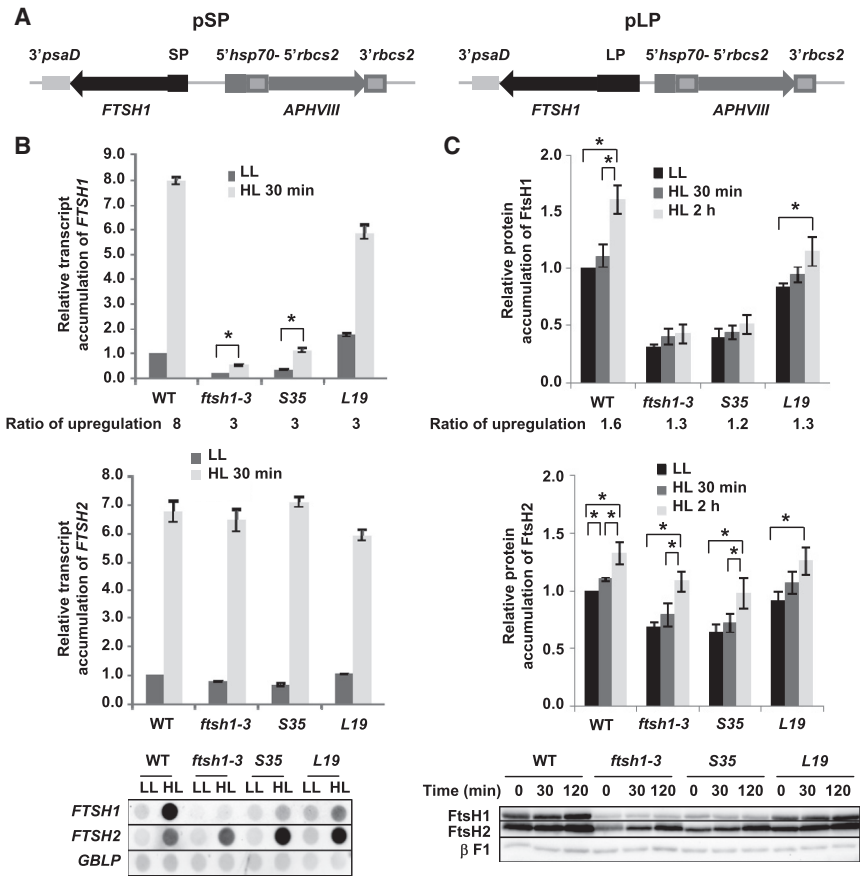

Figure 5. Regulation of *FTSH1* Expression Is Impaired by Promoter Truncations.

(A) Schematic map of the pSP and pLP plasmids used for complementation. The *FTSH1* gene is respectively expressed from the short promoter region remaining after the insertion of *TOC1* (SP), or from a larger promoter encompassing 500 bp upstream of the *FTSH1* translation start codon (LP). The *APHVIII* gene allows selection of transformants on paromomycin-supplemented plates.

(B) Accumulation of *FTSH1* and *FTSH2* transcripts determined by real-time qPCR in WT and *ftsh1*-3 strains as in representative clones from the transformation of the *ftsh1-3* strain with the pSP (*S35*) or pLP (*L19*) constructs. These strains were grown either under LL, or transferred to HL (1000 μmol photons m^{-2} s^{-1}) for 30 min. Transcript accumulation was normalized to that of the reference gene *GBLP*. Data represent means ± SD of six independent experiments. The asterisk indicates a value of $P < 0.05$ for a comparison of *FTSH1* transcript in *ftsh1-3* and *S35* strains between time 0 and time 30 min. Accumulation of the *FTSH1* and *FTSH2* transcripts was also detected by dot blots in the same samples as shown in the lower panel.

(C) Accumulation of FtsH1 and FtsH2 proteins was quantified by immunodetection in whole-cell protein extracts from the same strains, grown either under LL, or shifted to HL for 30 min or 2 h. A typical immunoblot is shown in the lower part of the panel. β F1 provides a loading control. Data represent means ± SD of three independent experiments. The asterisk indicates a value of $P < 0.05$.

decreased accumulation of FtsH2 together with the almost complete loss in FtsH1 in the *ftsh1-3* mutant (Figure 5C) suggests that accumulation of FtsH1 and FtsH2 is in part, but in part only, a concerted process. The above observations raise the question of oligomerization state of FtsH2 when in excess of FtsH1 in *ftsh1-3* and prompted us to monitor the oligomerization state of FtsH subunits in these various strains and conditions. Thylakoid membranes from WT and *ftsh1-3* strains, solubilized with dodecyl-β-maltoside (DDM), were separated by two-dimensional blue native PAGE (BN-PAGE) and analyzed by immunoblotting (Figure 8 and Supplemental Figure 9). In the WT grown under LL (Figure 8) or darkness (Supplemental Figure 9), most FtsH1/2 subunits comigrated into large protein complexes (L) in the 1-MDa region, as evidenced by their comigration with PSII supercomplexes, while a minor fraction was found in much smaller complexes (S), at the position where heterodimers would be expected (Malnoë et al., 2014). After 2 h of HL (Figure 8), both large and small complexes increased in abundance with no particular evidence of a change in their relative ratio. In *ftsh1-3* strain grown in LL, the accumulation of the large complex decreased dramatically compared with the WT, reflecting the decreased accumulation of FtsH1, while the accumulation of FtsH2 in the (S) form increased. When *ftsh1-3* was shifted to HL, the large FtsH complex showed no significant increase, while the amount of subunit FtsH2 in the lower molecular weight region increased with respect to LL conditions (Figure 8). Thus, most of the FtsH2 subunits, whose accumulation is induced after 2 h of HL, cannot assemble into FtsH large hetero-oligomeric complexes because of the reduced accumulation of FtsH1. They remain stalled in small complexes in *ftsh1-3*, most likely FtsH2 homodimers. We noted an overaccumulation of D1 fragments, diagnostic of damaged and partially degraded D1 subunit, in strain *ftsh1-3* exposed to HL, as predicted from the reduced amount of functional FtsH protease. Similarly the reaction center core lacking CP43 (RC47), indicated by an arrow in Figure 8, and the PSII monomers strongly increased at the expense of PSII supercomplexes in that strain upon HL (Figure 8).

FtsH1 and FtsH2 Form Reversible Intermolecular Disulfide Bridges

The oligomerization of FtsH could be borne by post-translational changes of its constitutive subunits, prominent among which is the formation of disulfide bridges. We noted that alignment of FtsH protein sequences from *Chlamydomonas* (CrFtsH1 and CrFtsH2) and *Arabidopsis* (AtFtsH1/5 and AtFtsH2/8) reveals conserved cysteines in the Walker A and B motifs, but also cysteines specific for CrFtsH1 and CrFtsH2 (Supplemental Figure 10A). We thus investigated possible post-translational modifications on FtsH cysteines by diagonal 2D redox SDS–PAGE, according to Ströher and Dietz (2008). After alkylation of free thiol by iodoacetamide to prevent spontaneous oxidation, FtsH1 and FtsH2 migrated not only as monomers but also as dimers and oligomers on the diagonal on SDS–PAGE under non-reducing conditions (Figure 9A, left panel). Proteins

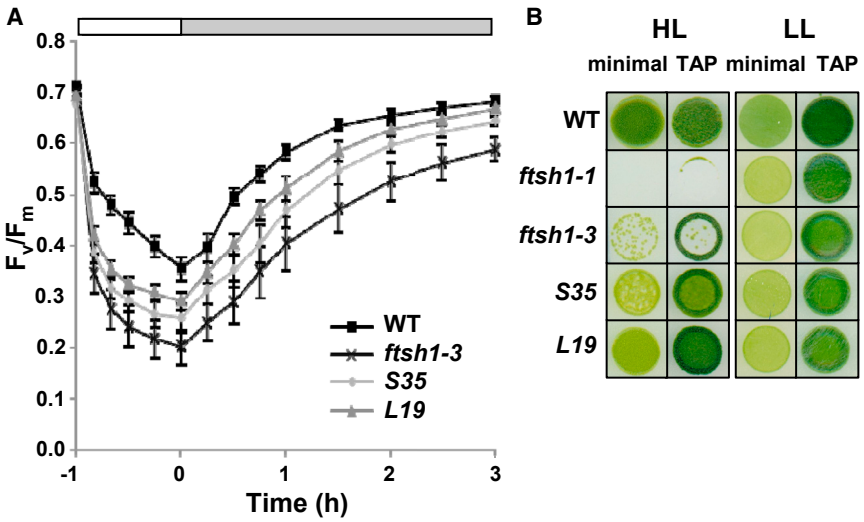

Figure 6. High Light Tolerance Decreases Proportionally with FtsH Protease Accumulation.

(A) PSII maximal photochemical efficiency (F_v/F_m), measured in WT, *ftsh1-3*, *S35*, and *L19* strains, grown to mid-log phase, transferred to HL for 1 h and then allowed to recover under LL for 3 h. FtsH1 levels at LL before transfer to HL were 1, 0.32, 0.40, and 0.84, respectively for WT, *ftsh1-3*, *S35*, and *L19* strains (see Figure 5C and Supplemental Table 1).

(B) Growth test of the same strains in phototrophic (minimal) and mixotrophic (TAP) conditions under HL or LL illumination for 5 days. The *ftsh1-1* strain expressing an inactive FtsH protease was included for comparison.

involved in intermolecular disulfide bridges should migrate below the diagonal when the second dimension is performed in reducing conditions. Indeed, FtsH dimers and oligomers released monomeric FtsH1 and FtsH2 below the diagonal after incubation of the gel strips under reducing conditions in the presence of 2-mercaptoethanol (Figure 9A, right panel). Proteins with intramolecular disulfide bridges may exhibit a slight change in electrophoretic mobility depending on the reducing conditions, thus migrating slightly out of diagonal when the second dimension is performed in reducing conditions. Although we did not observe such changes, it does not rule out the existence of intramolecular disulfide bridges that would affect only marginally the electrophoretic mobility of FtsH1 and FtsH2.

To confirm the presence of reversible disulfide bounds in FtsH, we analyzed the presence of oligomers of FtsH as a function of pre-treatments aimed at oxidizing or reducing the protein sulfhydryls/disulfides, using membrane protein extracts and Strep-tagged FtsH complexes. The latter were purified by affinity from an *ftsh1-3* strain complemented with an *FTSH1-Strep* construct (see Methods). We note that the oxidized forms increase upon extraction of the FtsH complexes (Figure 9B). Dimers and oligomers almost fully disappeared when membranes/complexes were incubated with a reducing compound such as dithiothreitol (DTT) before separation by non-reducing denaturing SDS–PAGE. They were formed again when membranes/complexes, treated with DDT, were subsequently incubated in the presence of a four-fold higher concentration of oxidizing compounds such as diamide and were dismantled again upon incubation with a five-fold excess (over diamide) of DTT (Figure 9B). We tentatively attribute the main FtsH oligomeric forms migrating with an apparent molecular mass (~171 kDa) to FtsH dimers, which are expected to have a molecular mass of ~140 kDa.

FtsH Proteolytic Activity Is Regulated by the Redox State

To determine whether FtsH proteolytic activity would be affected by the redox-controlled formation of intermolecular disulfide bridges, we assayed the proteolytic activity of the isolated Strep-tagged FtsH complex *in vitro* using β-casein as a substrate according to Lindahl et al. (2000). The activity of FtsH was estimated by the decrease of full-length β-casein. This activity is, as expected for an ATP-dependent FtsH protease, dependent on the addition of ATP in the reaction mixture (Figure 10A). The proteolytic activity of FtsH was then measured in various redox conditions (Figure 10B). The substrate β-casein was chosen because it has no cysteine residue, which could otherwise interfere with the experiment. A reducing treatment using 1 mM DTT strongly increased the FtsH proteolytic activity as measured by the extent of β-casein degradation, with FtsH even degrading partly itself, while an oxidizing treatment using 1 mM diamide inhibited proteolytic activity.

The evolution of FtsH disulfides upon HL was then tested *in vivo* (Figure 11). Cells grown in LL accumulate a significant amount of FtsH dimer (time 0 in Figure 11A). The ratio of dimers to monomeric FtsH1/2 decreased substantially within the first half hour of cell transfer to HL (Figure 11A). We tentatively assign this decrease in FtsH disulfides to activation of FtsH, as assayed *in vitro*, which would help to cope with the increased need for PSII repair in photoinhibitory conditions.

At longer time points under HL, FtsH1/2 and $FtsH_{di}$ both increased (Figure 11B), consistent with the light induction of FtsH expression we reported in Figure 1. We note an additional 40-kDa FtsH immunoreactive band, which may be an FtsH degradation product. Since the changes in ratio of dimers to monomeric FtsH1/2 that we observed at an early stage of HL treatment could arise from interconversion processes or to different proteolytic susceptibility of the proteins between the two states, we added cycloheximide, an inhibitor of cytosolic translation, at time 0 of the HL exposure to monitor the post-translational behavior of FtsH1 and FtsH2. As expected, cycloheximide prevented FtsH induction under HL (Figure 11B, right), thus allowing almost complete FtsH degradation after 4 h, as already shown in Figure 1C. It also allowed observation of a general decrease in the two forms of FtsH with time under HL (Figure 11B, right), which accounts for the increased degradation of FtsH that we observed in Figure 1C where samples were treated with DTT before SDS–PAGE. Thus, we

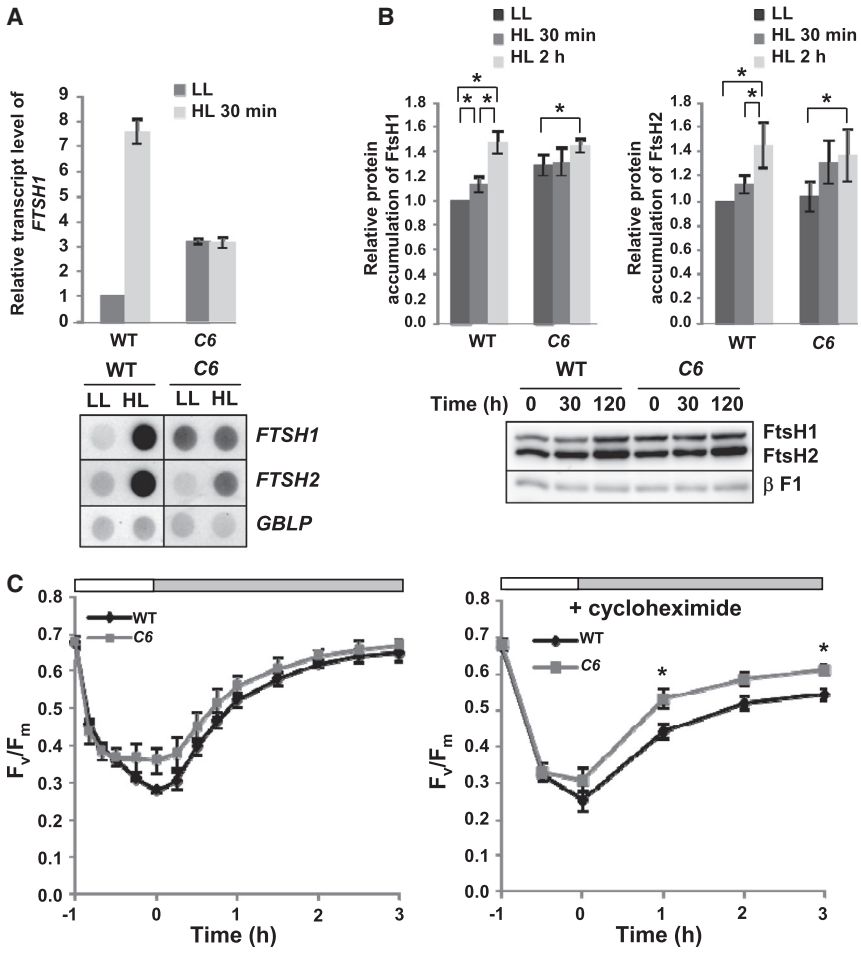

Figure 7. Overexpression of FtsH1 Confers Increased Photoprotection.

(A) Accumulation of *FTSH1* transcript in WT and overexpressing strain *C6*, analyzed as in Figure 5B. Means ± SD of six independent experiments are given. Dot-blot analysis of the same RNA samples, hybridized with *FTSH1*- and *FTSH2*-specific probes, is shown below the graph.

(B) Accumulation of FtsH1 and two proteins from the same cultures as in **(A)**, determined by immunoblots, a representative one being shown below the graphs. β F1 provides a loading control used for normalization. Data represent means ± SD of three independent experiments. The asterisk indicates a value of $P < 0.05$.

(C) PSII maximal photochemical efficiency (F_v/F_m), measured in the same strains grown in LL, transferred to HL for 1 h and allowed to recover under LL for 3 h, in the absence (left) or presence (right) of cycloheximide (30 μg ml^{-1}), added prior to the HL shift. Data represent means ± SD of five and three independent experiments for left and right, respectively. The asterisk indicates a value of $P < 0.05$ for a comparison between WT and *C6* strains.

found no evidence for a differential turnover of the dimeric and monomeric forms upon HL exposure. We noted, however, some interconversion of the monomeric form into the dimeric form of FtsH during the first hour of HL exposure in presence of cycloheximide, which could originate from the induction of ROS, which would oxidize FtsH subunits and thus promote oligomeric form, at the first stage of photoinhibition.

DISCUSSION

We previously described point mutations within the *FTSH1* gene that led to the accumulation of WT levels of an inactive FtsH protease (Malnoë et al., 2014). Here we obtained a distinct *ftsh1* mutant that displays 70% decreased accumulation of FtsH1 protein, because of a 5- to 15-fold decreased abundance of *FTSH1* mRNA, depending on light conditions (Supplemental Table 1), due to the insertion of a *TOC1* transposon in the *FTSH1* promoter region (Supplemental Figure 4). This phenotype offered a unique opportunity to address the behavior of FtsH2 when produced in excess over FtsH1, and the physiology of the HL control of FtsH expression.

FtsH Mainly Accumulates as Megacomplexes Independent of the Light Regime

FtsH-containing megacomplexes have been previously observed in *E. coli* (Kihara et al., 1996, 1998; Saikawa et al., 2004), yeast, or plant mitochondria (Steglich et al., 1999; Piechota et al., 2010). They contain prohibitin-like proteins, which would modulate FtsH proteolytic activity and its affinity for different substrates. Such megacomplexes were also observed in *Synechocystis* (Boehm et al., 2012), likely because of a transient or detergent-sensitive association with prohibitin-like proteins (Boehm et al., 2009; Sacharz et al., 2015). In our BN-PAGE experiments, where we used the 670-kDa PSII dimer and the 880- to 1400-kDa PSII supercomplexes (Caffarri et al., 2009) as molecular weight markers, we detected FtsH mainly in megacomplexes migrating with an apparent molecular mass of about 1 MDa, much larger than that expected for FtsH hexamers (~410 kDa). However, since to our knowledge prohibitin-like proteins have not been reported in chloroplasts, these FtsH megacomplexes should contain other interactants that require further identification.

We found no evidence for a susceptibility of these megacomplexes or of smaller FtsH complexes to shifts from LL to darkness or to HL conditions (Supplemental Figure 9 and Figure 8). This would be at variance with HL treatment of spinach thylakoids *in vitro* that was suggested to trigger the oligomerization of FtsH into active hexamers by acidification of the lumen (Yoshioka et al., 2010; Yoshioka and Yamamoto, 2011; Yoshioka-Nishimura et al., 2015), as reported for luminal Deg protease based on *in vitro* experiments showing its hexamerization upon acidification (Kley et al., 2011). We cannot exclude, however, more subtle changes in the composition of FtsH complexes that would not affect their migration upon BN-PAGE.

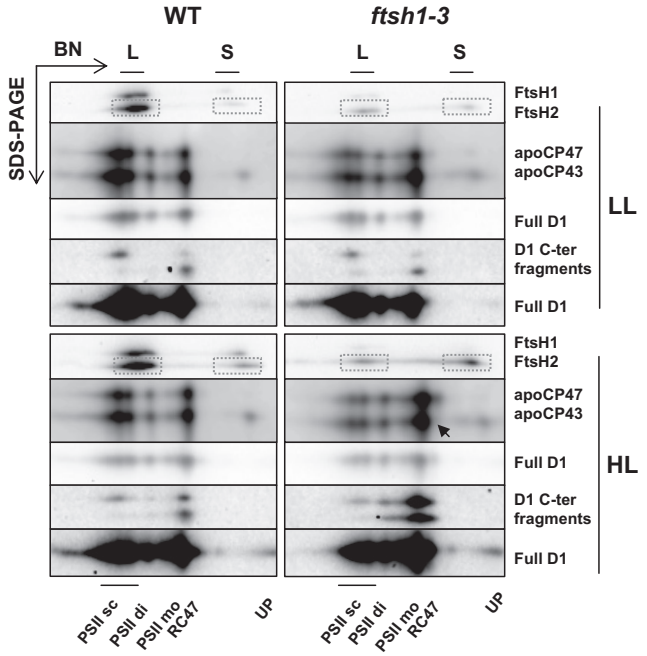

Figure 8. Concerted Accumulation of FtsH1 and FtsH2 in Large but Not Small Complexes.

Membrane proteins from WT and *ftsh1-3* strains grown under LL or transferred to HL for 2 h were solubilized by DDM and separated by blue native gel. The composition of the FtsH large (L) and small (S) complexes were analyzed in the second dimension by immunoblot. Full D1 and D1 C-terminal degradation fragments were immunodetected by D1 antibody against D1 C terminus. The positions of unassembled proteins (UP), reaction center core lacking CP43 as indicated by an arrow (RC47), monomers (PSII mo), dimers (PSII di), and supercomplexes (PSII sc) of PSII are indicated and were used as molecular mass markers. An overexposed D1 blot is shown at the bottom of each panel, as it reveals the position of unassembled D1 subunit.

FtsH2 Accumulates in Small Complexes when Produced in Excess over FtsH1

The *ftsh1-3* mutant offered the possibility to study the behavior of FtsH2 when produced in large excess over FtsH1 (Supplemental Table 1). We observed that the accumulation of FtsH2 in small complexes increased while the abundance of the large complexes decreased, supporting their obligatory hetero-oligomeric structure (Figure 8). The lack of stable FtsH2 homohexamers is consistent with the essential roles of both type A and B isoforms in *Arabidopsis* thylakoids (Yu et al., 2004, 2005; Zaltsman et al., 2005b) and the calculated thermodynamic stability (Moldavski et al., 2012). Assuming FtsH proposed cleavage sites by the thylakoid processing peptidase in higher plants (Rodrigues et al., 2011), *Chlamydomonas* FtsH2 mature protein would be smaller than that of FtsH1 (respectively 67 and 69 kDa). We tentatively attribute the FtsH smaller complexes, which migrate between PSII monomer (335 kDa) and unassembled D1 (38 kDa), to FtsH1/2 heterodimers in the WT. Some of the slightly smaller complexes in the *ftsh1-3* mutant then would correspond to FtsH2 homodimers. However, some of these complexes may be also accounted for by the interaction of FtsH2 with chloroplast chaperones recognizing misfolded proteins (Trösch et al., 2015).

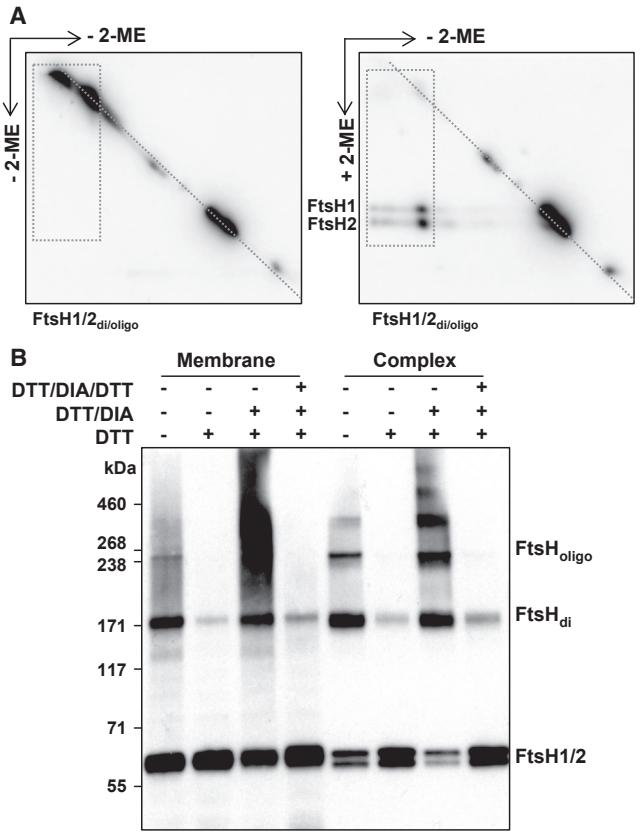

Figure 9. Existence and Redox Control of FtsH1 and FtsH2 Intermolecular Disulfide Bridges.

(A) FtsH1 and FtsH2 intermolecular disulfides *in vivo*. Membrane proteins isolated from WT cells were treated with cysteine alkylating agent iodoacetamide to prevent disulfide formation and separated by denaturating 2D redox 7% SDS–PAGE in the presence of 8 M urea (first dimension, no 2-mercaptoethanol treatment (− 2-ME); second dimension, + or − 2-ME). FtsH1 and FtsH2 were localized by immunoblot analysis. The diagonal along which proteins without disulfide bond are expected to lie is indicated by a dotted line.

(B) FtsH1 and FtsH2 disulfide formation is decreased by reduction, and reversibly increased by oxidation. Membrane proteins (left) or purified FtsH–Strep complexes (right) were pretreated for 15 min by 1 mM dithiothreitol (DTT), then incubated with 4 mM diamide for 15 min (DTT/DIA), and finally treated again with 20 mM DTT for 15 min (DTT/DIA/DTT). Control: no addition. The different FtsH forms were separated on 3%–8% Tris–acetate gel and detected by immunoblot. The positions of molecular weight markers are indicated. The FtsH oligomeric form migrating around 171 kDa is tentatively attributed to FtsH dimer ($FtsH_{di}$).

Increased Turnover of FtsH in High Light Condition Is Partly Compensated by Higher Level of *FTSH* Transcription

In eukaryotes, FtsH proteases are key players in the quality control of organelle proteins (Janska et al., 2013), the latter being highly exposed to oxidative damage because of the redox activity of electron transfer chains in mitochondria or chloroplasts. In chloroplasts, HL triggers the formation of ROS and damages the subunits of the photosynthetic complexes. As extensively described (reviewed in Kato and Sakamoto, 2009; Nixon et al., 2010), FtsH controls the repair of PSII upon photoinhibition via the degradation of damaged D1. Here, we

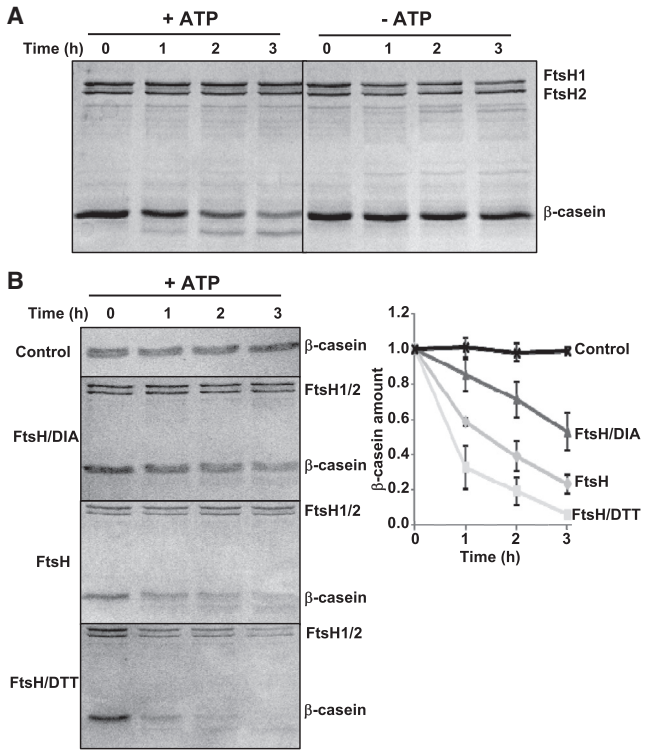

Figure 10. Proteolytic Activity of FtsH Is Activated by Reduction and Inhibited by Oxidation.

(A) ATP-dependent degradation of β-casein by purified FtsH–Strep complexes *in vitro*. Five micrograms of β-casein and 5 μg of FtsH–Strep were incubated at 37°C with (left) or without (right) addition of ATP. Samples taken from different time points (indicated on the top) were resolved by 10% SDS–PAGE and stained with Coomassie blue.

(B) Redox-controlled degradation *in vitro* of β-casein by purified FtsH–Strep complexes. Five micrograms of β-casein and 5 μg of FtsH–Strep complexes, pretreated on ice for 15 min with no addition (FtsH) or 1 mM DTT (FtsH/DTT) or 1 mM diamide (FtsH/DIA), were incubated at 37°C in the presence of ATP. Control was performed in the absence of added FtsH–Strep. Graph showing the relative amount of β-casein presents means ± SD of two independent experiments.

showed that HL upregulates the expression of *FTSH* genes in *Chlamydomonas*, at both the transcript and protein levels. While *FTSH* transcripts peak 30 min after the switch to HL, FtsH proteins increase more progressively for at least 4 h, pointing to additional post-transcriptional controls of the accumulation of the two subunits. Indeed, the half-life of FtsH1 and FtsH2 were much shortened in HL (Figure 1C). In these circumstances, the protease is likely exposed to harmful radicals, damaging the protease and leading to its proteolytic disposal. In *Arabidopsis*, HL also upregulates the accumulation of transcripts encoding *FTSH* genes (from three-fold for *FTSH1* to almost 20-fold for *FSTH8*), and nevertheless leads to a 40% drop in the protease abundance 30 min after exposure to HL (Sinvany-Villalobo et al., 2004; Zaltsman et al., 2005a).

The Amount of FtsH Is Limiting for the PSII Repair Cycle

Based on the contrasted abundance of FtsH in our mutants or complemented strains, we demonstrated that the amount of FtsH in thylakoid membranes is limiting for the repair of PSII. The more FtsH protease is in the thylakoid membrane, the less

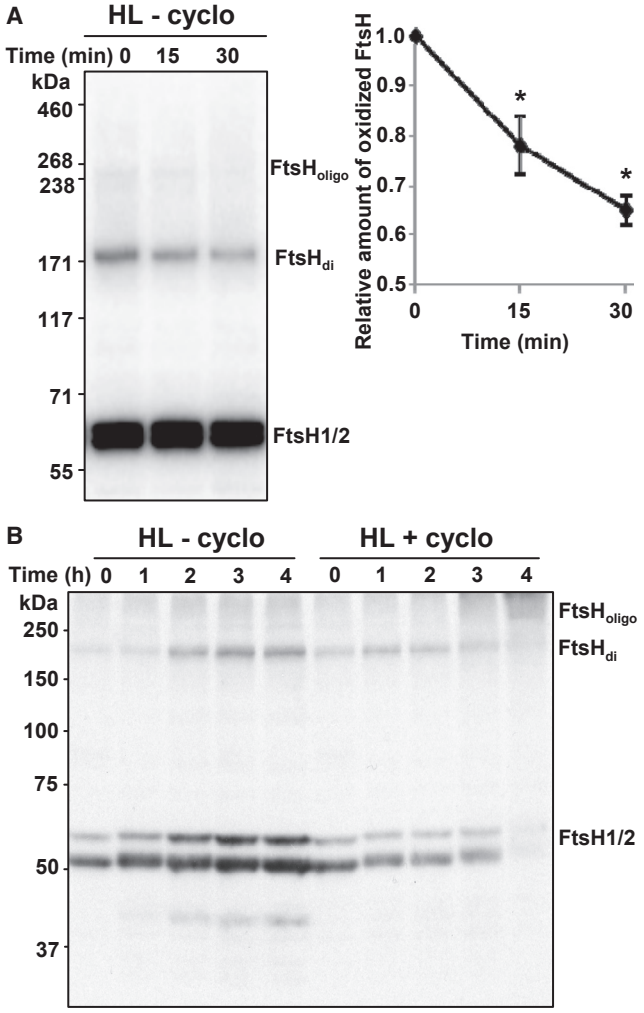

Figure 11. FtsH Intermolecular Disulfides *In Vivo* Upon High Light Illumination.

Membrane proteins isolated from WT cells following transfer to HL (1000 μmol photons m^{-2} s^{-1}) were treated with iodoacetamide to prevent artifactual disulfide formation and separated by non-reducing SDS–PAGE. Samples of membrane proteins were loaded on an equal chlorophyll basis. The accumulation of the different forms of FtsH1 and FtsH2 was followed by immunodetection in the samples harvested at the indicated time points. The positions of molecular weight markers are indicated.

(A) Intermolecular FtsH disulfides decrease during early stage of HL treatment. Membrane proteins were separated by 3%–8% SDS–PAGE on Tris–acetate gel. Relative amount of oxidized FtsH was expressed as the ratio of $FtsH_{di}$ over FtsH1/2. Data represent means ± SD of two independent experiments. The asterisk indicates a value of $P < 0.05$ for a comparison between time 0 and time 15 or 30 min.

(B) FtsH1/2 and $FtsH_{di}$ both increase upon long HL exposure in absence of cycloheximide while an immunochase experiment in the presence of cycloheximide shows some conversion of FtsH1/2 to $FtsH_{di}$ followed by the degradation of both forms of FtsH. Cycloheximide (30 μg ml^{-1}), an inhibitor of cytosolic translation, was added or not to an exponentially growing culture of WT cells under LL, just before the transfer to HL. Membrane proteins were separated on 7% SDS–PAGE in the presence of 8 M urea and immunodetected with FtsH antibody.

is the inactivation of PSII under HL and the faster is its recovery upon return to LL (Figures 6A and 7C). Together, these observations argue against a diffusion mechanism whereby FtsH would visit a number of sites for D1 degradation. If the mechanism of quality control of PSII by FtsH excludes that each proteolytic chamber of FtsH would contribute to the repair of many damaged PSII centers, a bimolecular mechanism in which a rather long-lived complex between FtsH and a PSII complex under repair should be considered for further kinetic characterization. The thylakoid FtsH isoforms differ in abundance (Sinvany-Villalobo et al., 2004; Yu et al., 2004), and are (based on our Coomassie staining) much less abundant than the major photosynthetic proteins, closer to the abundance of other auxiliary proteins in the thylakoid membranes (reviewed by Pribil et al., 2014). The limited access of FtsH to damaged PSII due to thylakoid stacking, even though partial unstacking is observed upon HL exposure (Fristedt et al., 2009; Puthiyaveetil et al., 2014), probably contributes to our observation that FtsH abundance is nevertheless limiting for protection against photoinhibition.

Redox Regulation of FtsH in *Chlamydomonas*

As mentioned above, a striking feature of FtsH in photoinhibitory conditions is its increased turnover. Although FtsH phosphorylation has been reported (Wang et al., 2014; Szyszka-Mroz et al., 2015), we detected no FtsH phosphorylation by immunodetection in our experimental conditions. FtsH subunits were also found in the nitrosylome of *Chlamydomonas* (Morisse et al., 2014), which suggests they are oxidative stress sensitive, a feature that may trigger their degradation. Indeed, excess light leads to the over-reduction of the electron transport chain and to the generation of ROS and/or RNS, causing redox changes at the protein level, which may contribute to protease activation, inhibition, or degradation. There are several recent studies on the role of oxidative modifications of proteases (Pérez-Pérez et al., 2014; Risør et al., 2014; Nishii et al., 2015). However, the possibility that the proteolytic activity of FtsH would be redox controlled had not yet been considered. In this study, we found unprecedented evidence for a sulfhydryl/disulfide redox regulation of FtsH oligomerization and proteolytic activity both *in vitro* and *in vivo*. Based on our present data, we conclude that the proteolytic activity of FtsH increases *in vitro* when disulfide bridges that promote the oligomeric state of the protease are reduced to sulfhydryls. The 30% decrease in DTT-sensitive FtsH oligomers that we detected *in vivo* upon the first 30 min of HL (Figure 11A) thus would correspond to an FtsH activation, as a primary response to cope with a sudden increase in PSII photodamage. The inactive FtsH fraction, although limited, could offer an easily accessible protease pool for PSII repair upon HL shift. The cleavage of the disulfide bridge *in vivo* could be controlled by membrane or stromal thioredoxins, since all cysteines of CrFtsH, most of them being conserved in AtFtsH, are on the stromal side (Supplemental Figure 10). It is noteworthy that there is only one cysteine in *Synechocystis* FtsH2/3. In *Arabidopsis*, FtsH2 and FtsH8 were found to be putative targets of HCF164, a membrane-anchored thioredoxin-like protein, but this is not likely to be the case *in vivo* since the active cysteine pair of HCF164 faces the lumen (Motohashi and Hisabori, 2006). CrFtsH1 and CrFtsH2 contain respectively four and three cysteines that could potentially form disulfide bridges. However, it is difficult to predict which cysteines of CrFtsH1/2 heterohexamers may form intermolecular disulfides from FtsH three-dimensional structures, since three-dimensional structures do not show protein dynamics and are only available for the soluble FtsH domain of bacterial homohexamers in which cysteines are closer within than between subunits (see FtsH crystal structure [Bieniossek et al., 2009] in Supplemental Figure 10B). We note that most of those cysteines that might be redox modified, lie in the FtsH ATPase/chaperone domain, facing the membrane on the stromal side and controlling the access to the proteolytic chamber (Supplemental Figure 10). At variance with the proteolytic sites, which can substitute one for another (Zhang et al., 2010), the chaperone sites act synergistically (Malnoë et al., 2014) and are good candidates for regulatory domains.

METHODS

Strains and Growth Conditions

WT derived from 137C (CC-5100 mt− and CC-5101 mt+), and mutant *Chlamydomonas* strains used in this report were grown in liquid medium to exponential phase at 2 × 10^6 cells ml^{-1} at 25°C, in TAP or minimal medium lacking acetate (Harris, 1989), under continuous light. Light intensity was set to 1000 μmol photons m^{-2} s^{-1} for HL or 10 μmol photons m^{-2} s^{-1} for LL. *Chlamydomonas* mutants have been described previously: *ccb4* (Kuras et al., 1997, 2007), *ftsh1-1* (Malnoë et al., 2014). Crosses were performed as described in Harris (1989). For growth tests on solid medium, exponentially growing cells were resuspended in water (2 × 10^5 cells ml^{-1}) and deposited as drops on TAP or minimal agarose plates. Photoinhibition was assessed by transferring cultures, grown to the exponential phase in TAP under LL, to HL for 1 h, and allowing them to subsequently recover under LL for several hours. NO variations were induced according to Wei et al. (2014). Cells were treated 30 min with 0.1 mM GSNO (*S*-nitrosoglutathione from BioVision) as NO donor, and 0.1 mM cPTIO (carboxy-PTIO, 2-(4-carboxyphenyl)-4,4,5,5-tetramethylimidazoline-1-oxyl-3-oxide from Sigma-Aldrich) as NO scavenger. In the case of HL and cPTIO treatment, cells grown under LL conditions were transferred to HL immediately after adding cPTIO.

Chlorophyll Fluorescence Analysis

Fluorescence-based photosynthetic parameters were measured at room temperature, on exponentially growing cultures that were dark-adapted for 1 min. Two fluorescence systems were used: a home-made fluorescence setup (Rappaport et al., 2007) whereby the detecting light is 532 nm for measurements on 1-ml aliquots of liquid cultures, or a fluorescence imaging system (BeamBio, SpeedZen camera; Johnson et al., 2009) whereby the detecting light is blue for measurements on plates. In both setups the saturating pulse is a 250-ms pulse of green light (532 nm, 6200 and 2600 μmol photons m^{-2} s^{-1}, respectively). The maximal quantum yield of PSII photochemistry (F_v/F_m) was calculated as $(F_m - F_0)/F_m$, where F_v is the variable fluorescence, F_0 is the fluorescence level measured after cells' dark adaptation, and F_m is the maximum fluorescence level after the saturating light pulse (Genty et al., 1989; Baker, 2008). We checked that the detecting light was weak enough to avoid any actinic effect, which would result in an overestimation of F_0. The samples were not CO_2 supplemented.

Map-Based Cloning of *Su$_{4\text{-}ccb4}$*

The *Su$_{4\text{-}ccb4}$* mutant was crossed to the interfertile strain S1-D2 that shows a profusion of polymorphisms with current *C. reinhardtii* laboratory strains (Gross et al., 1988; Rymarquis et al., 2005; Gallaher et al., 2015); 152 zygotes were dissected and 64 complete tetrads recovered. Mutants were identified among the resulting 403 progenies by their lower F_v/F_m values after a 1-h HL. The *Su$_{4\text{-}ccb4}$* phenotype of the 218

mutant progenies selected this way was further confirmed by immunodetection of the FtsH1 protein. For linkage analysis, PCR reactions were performed on all 403 progenies with primer combinations generating PCR products of different size from the *FTSH1* gene of *C. reinhardtii* (primers FTSH1-S1 and FTSH1-A9, 449 bp) or of its S1-D2 counterpart (FtsH1-S1 and FtsH1-AS1D2, 308 bp). Oligonucleotides used in this study are listed in Supplemental Table 2.

Plasmid Construction and Transformation

Plasmid pSL18-g*FTSH1* carrying both a paromomycin cassette resistance and the *FTSH1* coding sequence cloned between the *PSAD* promoter and 5′ UTR regions and the *PSAD* 3′ UTR, including the polyadenylation site, has been described in Malnoë et al. (2014). Plasmids pSL18-g*FTSH1-proS* (pSP) and pSL18-g*FTSH1-proL* (pLP) carrying the *FTSH1* gene expressed from the short and longer truncated versions of the *FTSH1* promoter were constructed by *PSAD* promoter replacement. PCR fragments, amplified from cloned *FTSH1* genomic DNA with primers FTSH1-proS-S/FTSH1-exon2-A or FTSH1-proL-S/FTSH1-exon2-A, were digested by *Xho*I and *Pfo*I and cloned into the 7.7-kb *Xho*I/*Pfo*I fragment from vector pSL18-g*FTSH1* (prepared in *dam*−/*dcm*− *E. coli* strain, the restriction enzyme *Pfo*I being sensitive to methylation). Plasmids were linearized or not with *Acl*I prior to transformation into strain *ftsh1-3* by an electroporation method (Shimogawara et al., 1998), using the parameters 10 μF and 1000 V cm^{-1}. Transformants were selected on TAP medium supplemented with paromomycin (5 μg ml^{-1}), and screened on TAP medium without paromomycin by fluorescence measurements (F_v/F_m after 2 h of HL). Transformants with the short and longer truncated versions of the *FTSH1* promoters were screened for full *FTSH1* insertion by PCR amplification of their genomic DNA with primers pSL18-S1b (before the promoter cloning site *Xho*I) and pSL18-A2 (in the end of 3′-*PSAD*) for products of 4.2 kb and 4.6 kb, respectively. The expression of FtsH1 was detected by immunodetection.

Whole-Genome Sequencing

Around 10 μg of high-quality DNA ($OD_{260}/OD_{280} \sim 1.8$ and no detectable material below 17 kb) were extracted from strains *ccb4* and *Rccb4-SR1* using a DNeasy plant maxi kit (Qiagen). Library generation using the TrueSeq nano DNA method and whole-genome shotgun sequencing using the Illumina short-read technology (HiSeq 2500 instrument) with Paired-End (2 × 100 nt, insert size ~300 bp) were performed by Tufts University core facility. About 180 million read pairs were generated. Reads were aligned as described in Boulouis et al. (2015), on the *C. reinhardtii* reference genome (Phytosome V5.5) using the genomics workbench and sequence viewer software available at our institute bioinformatics server.

Nucleic Acid Analysis

For Southern blot, genomic DNA was isolated by a DNeasy Plant Mini Kit (Qiagen), digested by *Sac*I or *Pvu*I, electrophoresed on 0.8% agarose gel, and blotted as described by Sambrook and Russell (2001). Relevant DNA fragments were detected by hybridization with digoxin-labeled probes and synthesized by PCR using digoxin-labeled dNTPs (Roth). For RNA blot, total RNAs from *Chlamydomonas* were extracted with TRI reagent (Sigma). Ten micrograms of total RNA were separated on 1.0% denaturing agarose–formaldehyde gels, transferred to Nylon$^+$ membrane (Roth), and fixed by UV light crosslinking (UV Crosslinker, UVC 500, Hoefer). For dot blot, 1 μg of total RNA treated with DNase I (NEB) was loaded onto Nylon$^+$ membrane (Roth) using the Whatman Minifold Dot-blot system. Target transcripts were detected with digoxin-labeled probes.

Quantitative Real-Time PCR

One microgram of total RNA, isolated from *Chlamydomonas* cells with TRI reagent (Sigma) and treated with DNase to avoid amplification of genomic DNA (as controlled by the size and melting curves of PCR products), was reverse transcribed into cDNA with the SuperScript III Reverse Transcriptase kit (Life Technologies) using random primer mix or oligo(dT)20, according to the supplier protocol. Real-time qPCR was performed on a Bio-Rad CFX96 detection system using SsoAdvanced Universal SYBR Green Supermix (Bio-Rad) and the primers listed in Supplemental Table 2. All reactions were run in triplicate in three independent technical repeats and two independent biological repeats, and data represent means ± SD of these six independent experiments. Relative transcript levels of *FTSH* genes were calculated by the ΔΔCP (crossing point) method based on PCR efficiency (*E*) as described in Pfaffl (2001) and normalized to the accumulation of the reference gene Cre06.g278222 (GBLP) encoding the *Chlamydomonas* G protein β-subunit-like polypeptide (Schloss, 1990; Im and Grossman, 2002; Maruyama et al., 2014). Real-time PCR efficiency of each pair of primers was determined according to the equation $E = 10[-1/\text{slope}]$, and the slope was calculated by plotting CP against the logarithmic values of tenfold serial dilutions (Pfaffl, 2001).

Protein Isolation and Immunoblot Analysis

Whole-cell protein extraction, denaturing SDS–PAGE, transfer, and immunodetection were performed according to Malnoë et al. (2014). Cell extracts were loaded on chlorophyll basis and separated by electrophoresis on 8% SDS–polyacrylamide gels in the presence of 8 M urea, except when indicated differently. Proteins were transferred onto a polyvinylidene fluoride membrane (0.22 μm, GE Healthcare) by semidry method. Antibodies against FtsH1, FtsH2, CP47, CP43, and D1 C terminus (Malnoë et al., 2014), cytochrome *f*, cytochrome b_6, and subunit IV (Kuras and Wollman, 1994; de Vitry et al., 2004), CCB2 and CCB4 (Kuras et al., 2007), and the β-subunit of mitochondrial (β F1) or chloroplast (β CF1) ATP synthase (Atteia et al., 1992) have been previously described. Antibodies against peptides of *Chlamydomonas* specific for FtsH1 and FtsH2 (Malnoë et al., 2014) were used at a 1:5000 dilution (Figures 1B, 3B, and 4B; Supplemental Figures 3B and 6B). Antibody against *Arabidopsis* FtsH2 (Qi et al., 2016), generously provided by Fei Yu, that cross-reacts with FtsH1 and FtsH2 in *Chlamydomonas* was used at a 1:10 000 dilution (Figures 1C, 5C, 7B, and 8–11; Supplemental Figures 8A and 9B). We quantified the content in FtsH1 and FtsH2 by immunoblot chemiluminescence detection with a ChemiDoc XRS+ camera (Bio-Rad) using β F1 as loading control.

BN-PAGE

BN-PAGE analyses were essentially performed according to Malnoë et al. (2014). Cells from a 100-ml of culture (2 × 10^6 cells ml^{-1}) were collected by centrifugation, resuspended in 1 ml of HM buffer (10 mM HEPES [pH 7.5], 5 mM $MgCl_2$), and sonicated three times on ice by 10-s 75-W pulses, spaced by 1 min. Membrane fraction was collected from the cell lysates by ultracentrifugation in a TLA100.2 rotor (Beckman) at 279 000 *g* at 4°C for 10 min. Membranes were resuspended in 25BTH20G buffer (25 mM Bis-Tris-HCl [pH 7.0], 20% [w/v] glycerol) at the same protein concentration, which corresponded to a final chlorophyll concentration of 2 mg ml^{-1} for the WT and 1.2 mg ml^{-1} for *ftsh1-3*. Membranes were then solubilized by adding one volume of 2% (w/v) dodecyl-β-maltoside (DDM, D310LA Anatrace) for 10 min on ice, and supernatant was collected after centrifugation at 16 110 *g* for 10 min at 4°C. Five microliters of supernatant from each sample was complemented with 0.5 μl of 10× loading buffer (100 mM Bis-Tris [pH 7.0], 0.5 M aminocaproic acid, 5% Coomassie brilliant blue G250, 30% sucrose) and loaded on a precast 3%–12% NativePAGE Bis-Tris gel (Life Technologies, BN2011X10). Electrophoresis was performed with a cathode buffer (50 mM tricine, 15 mM Bis-Tris [pH 7.0], and 0.04% Coomassie brilliant blue G250) and anode buffer (50 mM Bis-Tris [pH 7.0]) for 20 min at 50 V and then 2 h at 150 V. For the denaturing second-dimension analysis, strips cut from the first-dimension gel were incubated at room temperature for 15 min in 2% SDS, 66 mM Na_2CO_3,

and 0.67% β-mercaptoethanol, and applied to 8% SDS–polyacrylamide gels containing 8 M urea.

Diagonal 2D Redox SDS–PAGE and Non-reducing SDS–PAGE

Diagonal 2D redox SDS–PAGE was performed as described in Ströher and Dietz (2008). Isolated membrane fractions (same procedure as for BN-PAGE) were resuspended in HM buffer to a final chlorophyll concentration of 1 mg ml^{-1}, then incubated at 4°C in the dark for 30 min in the presence of 100 mM iodoacetamide to block all free thiols and prevent thiol reshuffling during the subsequent steps. First dimension of non-reducing SDS–PAGE was performed by electrophoresis on 7% SDS–polyacrylamide gel containing 8 M urea. For Diagonal 2D PAGE, gel strips cut from the first dimension of non-reducing SDS–PAGE were incubated for 15 min at room temperature in denaturing buffer (2% SDS, 66 mM Na_2CO_3) with or without 0.67% β-mercaptoethanol and applied on 7% SDS–polyacrylamide gel containing 8 M urea. Non-reducing SDS–PAGE was performed by electrophoresis on 7% SDS–polyacrylamide gel containing 8 M urea with molecular weight markers (Precision Plus Protein Dual Xtra standards, Bio-Rad) or on precast 3%–8% Tris–acetate gel (Novex, NuPAGE 3%–8% Tris–Acetate Gel, Life Technologies EA0375BOX) with molecular weight markers (HiMark Pre-Stained Protein Standard, Life Technologies).

Proteolytic Activity Assay of FtsH Against β-Casein

FtsH–Strep complexes, carrying a *Strep*-tag II (Schmidt and Skerra, 2007) fused to the C-terminal end of FtsH1, were purified by affinity using StepTactin columns (GE Healthcare StrepTrap HP, 28-9075-46). The amount of FtsH in the eluate was determined by SDS–PAGE and Coomassie brilliant blue R250 staining. When indicated, purified FtsH–Strep complexes were incubated for 15 min on ice with 1 mM DTT or 1 mM diamide to either reduce or oxidize disulfide bridges. Degradation of protein substrate by FtsH was assayed as described in Asahara et al. (2000) with a few modifications. Reaction mixtures contained 2.1 μM β-casein (50 μg ml^{-1}) and 0.7 μM purified FtsH–Strep (50 μg ml^{-1}). Five micrograms of β-casein (Sigma-C6905, β-casein from bovine milk) of a stock 1 mg ml^{-1}, heated 3 min at 100°C and cooled at 37°C just before the experiment, was added to 100 μl of reaction mixtures (16 mM Tris-HCl [pH 8.0], 120 mM NaCl, 0.05% digitonin, 6.25 mM Tris–acetate [pH 8.0], 2.5 mM $MgCl_2$, 12.5 μM $ZnSO_4$, with or without 5 mM ATP, and with or without 5 μg of purified FtsH–Strep) and incubated at 37°C for 4 h. Aliquots (20 μl) were harvested at the indicated time points, separated by electrophoresis on reducing 10% SDS–polyacrylamide gels. Abundance of β-casein was determined by quantification using the Image Lab software (Bio-Rad) from a ChemiDoc (Bio-Rad) scan of the gel stained with Coomassie blue R250.

SUPPLEMENTAL INFORMATION

Supplemental Information is available at *Molecular Plant Online*.

FUNDING

This work was supported by basic funding from CNRS and UPMC, and grants ANR-07-BLAN-0114, ANR-12-BSV8-0011 (FtsH-Thyl-Chlamy), and ANR-11-LABX-0011 (DYNAMO).

AUTHOR CONTRIBUTIONS

F.W., F.-A.W., and C.V. designed the research. F.W., Y.Q., A.M., and C.d.V. performed the experiments. All authors analyzed the data and wrote the paper. C.d.V. coordinated the project.

ACKNOWLEDGMENTS

We thank Jacqueline Girard-Bascou for sharing her genetic expertise, Stéphane Lemaire and Christophe Marchand for sharing their redox-modification expertise, Nicolas Tourasse and Olivier Vallon for help with sequencing data analysis, and Fei Yu for *Arabidopsis* FtsH2 antibody. No conflict of interest declared.

Received: May 31, 2016
Revised: September 7, 2016
Accepted: September 17, 2016
Published: October 1, 2016

REFERENCES

Akiyama, Y., Yoshihisa, T., and Ito, K. (1995). FtsH, a membrane-bound ATPase, forms a complex in the cytoplasmic membrane of *Escherichia coli*. J. Biol. Chem. **270**:23485–23490.

Asahara, Y., Atsuta, K., Motohashi, K., Taguchi, H., Yohda, M., and Yoshida, M. (2000). FtsH recognizes proteins with unfolded structure and hydrolyzes the carboxyl side of hydrophobic residues. J. Biochem. **127**:931–937.

Atteia, A., de Vitry, C., Pierre, Y., and Popot, J.L. (1992). Identification of mitochondrial proteins in membrane preparations from *Chlamydomonas reinhardtii.* J. Biol. Chem. **267**:226–234.

Baker, N.R. (2008). Chlorophyll fluorescence: a probe of photosynthesis *in vivo*. Annu. Rev. Plant Biol. **59**:89–113.

Barth, J., Bergner, S.V., Jaeger, D., Niehues, A., Schulze, S., Scholz, M., and Fufezan, C. (2014). The interplay of light and oxygen in the reactive oxygen stress response of *Chlamydomonas reinhardtii* dissected by quantitative mass spectrometry. Mol. Cell. Proteomics **13**:969–989.

Bieniossek, C., Niederhauser, B., and Baumann, U.M. (2009). The crystal structure of apo-FtsH reveals domain movements necessary for substrate unfolding and translocation. Proc. Natl. Acad. Sci. USA **106**:21579–21584.

Boehm, M., Nield, J., Zhang, P., Aro, E.M., Komenda, J., and Nixon, P.J. (2009). Structural and mutational analysis of band 7 proteins in the cyanobacterium *Synechocystis* sp. strain PCC 6803. J. Bacteriol. **191**:6425–6435.

Boehm, M., Yu, J., Krynicka, V., Barber, M., Tichy, M., Komenda, J., Nixon, P.J., and Nield, J. (2012). Subunit organization of a *Synechocystis* hetero-holigomeric thylakoid FtsH complex involved in PSII repair. Plant Cell **24**:3669–3683.

Boulouis, A., Drapier, D., Razafimanantsoa, H., Wostrikoff, K., Tourasse, N.J., Pascal, K., Girard-Bascou, J., Vallon, O., Wollman, F.A., and Choquet, Y. (2015). Spontaneous dominant mutations in *Chlamydomonas* highlight ongoing evolution by gene diversification. Plant Cell **27**:984–1001.

Burgess, A.J., Retkute, R., Pound, M.P., Foulkes, J., Preston, S.P., Jensen, O.E., Pridmore, T.P., and Murchie, E.H. (2015). High-resolution three-dimensional structural data quantify the impact of photoinhibition on long-term carbon gain in wheat canopies in the field. Plant Physiol. **169**:1192–1204.

Caffarri, S., Kouøil, R., Kereïche, S., Boekema, E.J., and Croce, R. (2009). Functional architecture of higher plant photosystem II supercomplexes. EMBO J. **28**:3052–3063.

Chang, H.L., Hsu, Y.T., Kang, C.Y., and Lee, T.M. (2013). Nitric oxide down-regulation of carotenoid synthesis and PSII activity in relation to very high light-induced singlet oxygen production and oxidative stress in *Chlamydomonas reinhardtii*. Plant Cell Physiol. **54**:1296–1315.

Chen, M., Choi, Y., Voytas, D.F., and Rodermel, S. (2000). Mutations in the *Arabidopsis VAR2* locus cause leaf variegation due to the loss of a chloroplast FtsH protease. Plant J. **22**:303–313.

Day, A., and Rochaix, J.D. (1991). A transposon with an unusual LTR arrangement from *Chlamydomonas reinhardtii* contains an internal tandem array of 76 bp repeats. Nucleic Acids Res. **19**:1259–1266.

Day, A., Schirmer-Rahire, M., Kuchka, M.R., Mayfield, S.P., and Rochaix, J.D. (1988). A transposon with an unusual arrangement of long terminal repeats in the green alga *Chlamydomonas reinhardtii*. EMBO J. **7**:1917–1927.

de Vitry, C., Desbois, A., Redeker, V., Zito, F., and Wollman, F.A. (2004). Biochemical and spectroscopic characterization of the covalent binding of heme to cytochrome b_6. Biochemistry **43**:3956–3968.

Duanmu, D., Casero, D., Dent, R.M., Gallaher, S., Yang, W., Rockwell, N.C., Martin, S.S., Pellegrini, M., Niyogi, K.K., Merchant, S.S., et al. (2013). Retrograde bilin signaling enables *Chlamydomonas* greening and phototrophic survival. Proc. Natl. Acad. Sci. USA **110**:3621–3626.

Erickson, E., Wakao, S., and Niyogi, K.K. (2015). Light stress and photoprotection in *Chlamydomonas reinhardtii*. Plant J. **82**:449–465.

Fischer, B.B., Krieger-Liszkay, A., and Eggen, R.L. (2005). Oxidative stress induced by the photosensitizers neutral red (type I) or rose bengal (type II) in the light causes different molecular responses in *Chlamydomonas reinhardtii*. Plant Sci. **168**:747–759.

Fischer, B.B., Wiesendanger, M., and Eggen, R.I. (2006). Growth condition-dependent sensitivity, photodamage and stress response of *Chlamydomonas reinhardtii* exposed to high light conditions. Plant Cell Physiol. **47**:1135–1145.

Fischer, B.B., Ledford, H.K., Wakao, S., Huang, S.G., Casero, D., Pellegrini, M., Merchant, S.S., Koller, A., Eggen, R.I., and Niyogi, K.K. (2012). SINGLET OXYGEN RESISTANT 1 links reactive electrophile signaling to singlet oxygen acclimation in *Chlamydomonas reinhardtii*. Proc. Natl. Acad. Sci. USA **109**:E1302–E1311.

Fristedt, R., Willig, A., Granath, P., Crèvecoeur, M., Rochaix, J.D., and Vener, A.V. (2009). Phosphorylation of photosystem II controls functional macroscopic folding of photosynthetic membranes in *Arabidopsis*. Plant Cell **21**:3950–3964.

Gallaher, S.D., Fitz-Gibbon, S.T., Glaesener, A.G., Pellegrini, M., and Merchant, S.S. (2015). *Chlamydomonas* genome resource for laboratory strains reveals a mosaic of sequence variation, identifies true strain histories, and enables strain-specific studies. Plant Cell **27**:2335–2352.

Genty, B., Briantais, J.M., and Baker, N.R. (1989). The relationship between the quantum yield of photosynthetic electron transport and quenching of chlorophyll fluorescence. Biochim. Biophys. Acta **990**:87–92.

Gross, C.H., Ranum, L.P., and Lefebvre, P.A. (1988). Extensive restriction fragment length polymorphisms in a new isolate of *Chlamydomonas reinhardtii*. Curr. Genet. **13**:503–508.

Grossman, A.R., Catalanotti, C., Yang, W., Dubini, A., Magneschi, L., Subramanian, V., Posewitz, M.C., and Seibert, M. (2011). Multiple facets of anoxic metabolism and hydrogen production in the unicellular green alga *Chlamydomonas reinhardtii*. New Phytol. **190**:279–288.

Harris, E.H. (1989). The *Chlamydomonas* Sourcebook (San Diego: Academic Press).

Higo, K., Ugawa, Y., Iwamoto, M., and Korenaga, T. (1999). Plant cis-acting regulatory DNA elements (PLACE) database. Nucleic Acids Res. **27**:297–300.

Hudson, M.E., and Quail, P.H. (2003). Identification of promoter motifs involved in the network of phytochrome A-regulated gene expression by combined analysis of genomic sequence and microarray data. Plant Physiol. **133**:1605–1616.

Im, C.S., and Grossman, A.R. (2002). Identification and regulation of high light-induced genes in *Chlamydomonas reinhardtii*. Plant J. **30**:301–313.

Janska, H., Kwasniak, M., and Szczepanowska, J. (2013). Protein quality control in organelles-AAA/FtsH story. Biochim. Biophys. Acta **1833**:381–387.

Järvi, S., Suorsa, M., and Aro, E.M. (2015). Photosystem II repair in plant chloroplasts - regulation, assisting proteins and shared components with photosystem II biogenesis. Biochim. Biophys. Acta **1847**:900–909.

Johnson, X., Vandystadt, G., Bujaldon, S., Wollman, F.A., Dubois, R., Roussel, P., Alric, J., and Béal, D. (2009). A new setup for *in vivo* fluorescence imaging of photosynthetic activity. Photosynth. Res. **102**:85–93.

Kato, Y., and Sakamoto, W. (2009). Protein quality control in chloroplasts: a current model of D1 protein degradation in the photosystem II repair cycle. J. Biochem. **146**:463–469.

Kato, Y., Sun, X., Zhang, L., and Sakamoto, W. (2012). Cooperative D1 degradation in the photosystem II repair mediated by chloroplastic proteases in *Arabidopsis*. Plant Physiol. **159**:1428–1439.

Kapri-Pardes, E., Naveh, L., and Adam, Z. (2007). The thylakoid lumen protease Deg1 is involved in the repair of photosystem II from photoinhibition in *Arabidopsis*. Plant Cell **19**:1039–1047.

Kerchev, P., De Smet, B., Waszczak, C., Messens, J., and Van Breusegem, F. (2015). Redox strategies for crop improvement. Antioxid. Redox Signal. **23**:1186–1205.

Kihara, A., Akiyama, Y., and Ito, K. (1996). A protease complex in the *Escherichia coli* plasma membrane: HflKC (HflA) forms a complex with FtsH (HflB), regulating its proteolytic activity against SecY. EMBO J. **15**:6122–6131.

Kihara, A., Akiyama, Y., and Ito, K. (1998). Different pathways for protein degradation by the FtsH/HflKC membrane-embedded protease complex: an implication from the interference by a mutant form of a new substrate protein, YccA. J. Mol. Biol. **279**:175–188.

Kley, J., Schmidt, B., Boyanov, B., Stolt-Bergner, P.C., Kirk, R., Ehrmann, M., Knopf, R.R., Naveh, L., Adam, Z., and Clausen, T. (2011). Structural adaptation of the plant protease Deg1 to repair photosystem II during light exposure. Nat. Struct. Mol. Biol. **18**:728–731.

Komenda, J., Sobotka, R., and Nixon, P.J. (2012). Assembling and maintaining the Photosystem II complex in chloroplasts and cyanobacteria. Curr. Opin. Plant Biol. **15**:245–251.

Krieger-Liszkay, A., Kós, P.B., and Hideg, E. (2011). Superoxide anion radicals generated by methylviologen in photosystem I damage photosystem II. Physiol. Plant. **142**:17–25.

Krzywda, S., Brzozowski, A.M., Verma, C., Karata, K., Ogura, T., and Wilkinson, A.J. (2002). The crystal structure of the AAA domain of the ATP-dependent protease FtsH of *Escherichia coli* at 1.5 A resolution. Structure **10**:1073–1083.

Kuras, R., de Vitry, C., Choquet, Y., Girard-Bascou, J., Culler, D., Büschlen, S., Merchant, S., and Wollman, F.A. (1997). Molecular genetic identification of a pathway for heme binding to cytochrome b_6. J. Biol. Chem. **272**:32427–32435.

Kuras, R., Saint-Marcoux, D., Wollman, F.A., and de Vitry, C. (2007). A specific *c*-type cytochrome maturation system is required for oxygenic photosynthesis. Proc. Natl. Acad. Sci. USA **104**:9906–9910.

Kuras, R., and Wollman, F.A. (1994). The assembly of cytochrome b_6/f complexes: an approach using genetic transformation of the green alga *Chlamydomonas reinhardtii*. EMBO J. **13**:1019–1027.

Langklotz, S., Baumann, U., and Narberhaus, F. (2012). Structure and function of the bacterial AAA FtsH protease. Biochim. Biophys. Acta **1823**:40–48.

Lindahl, M., Spetea, C., Hundal, T., Oppenheim, A.B., Adam, Z., and Andersson, B. (2000). The thylakoid FtsH protease plays a role in the light-induced turnover of the photosystem II D1 protein. Plant Cell **12**:419–431.

Malnoë, A., Wollman, F.A., de Vitry, C., and Rappaport, F. (2011). Photosynthetic growth despite a broken Q-cycle. Nat. Commun. **2**:301.

Malnoë, A., Wang, F., Girard-Bascou, J., Wollman, F.A., and de Vitry, C. (2014). Thylakoid FtsH protease contributes to photosystem II and cytochrome b_6f remodeling in *Chlamydomonas reinhardtii* under stress conditions. Plant Cell **26**:373–390.

Maruyama, S., Tokutsu, R., and Minagawa, J. (2014). Transcriptional regulation of the stress-responsive light harvesting complex genes in *Chlamydomonas reinhardtii*. Plant Cell Physiol. **55**:1304–1310.

Merchant, S.S., Kropat, J., Liu, B., Shaw, J., and Warakanont, J. (2012). TAG, you're it! *Chlamydomonas* as a reference organism for understanding algal triacylglycerol accumulation. Curr. Opin. Biotechnol. **23**:352–363.

Moldavski, O., Levin-Kravets, O., Ziv, T., Adam, Z., and Prag, G. (2012). The hetero-hexameric nature of a chloroplast AAA+ FtsH protease contributes to its thermodynamic stability. PLoS One **7**:e36008.

Morisse, S., Zaffagnini, M., Gao, X.H., Lemaire, S.D., and Marchand, C.H. (2014). Insight into protein S-nitrosylation in *Chlamydomonas reinhardtii*. Antioxid. Redox Signal. **21**:1271–1284.

Motohashi, K., and Hisabori, T. (2006). HCF164 receives reducing equivalents from stromal thioredoxin across the thylakoid membrane and mediates reduction of target proteins in the thylakoid lumen. J. Biol. Chem. **281**:35039–35047.

Murchie, E.H., Ali, A., and Herman, T. (2015). Photoprotection as a trait for rice yield improvement: status and prospects. Rice **8**:31.

Nishii, W., Kukimoto-Niino, M., Terada, T., Shirouzu, M., Muramatsu, T., Kojima, M., Kihara, H., and Yokoyama, S. (2015). A redox switch shapes the Lon protease exit pore to facultatively regulate proteolysis. Nat. Chem. Bio. **11**:45–51.

Niwa, H., Tsuchiya, D., Makyio, H., Yoshida, M., and Morikawa, K. (2002). Hexameric ring structure of the ATPase domain of the membrane-integrated metalloprotease FtsH from *Thermus thermophilus* HB8. Structure **10**:1415–1423.

Nixon, P.J., Michoux, F., Yu, J., Boehm, M., and Komenda, J. (2010). Recent advances in understanding the assembly and repair of photosystem II. Ann. Bot. **106**:1–16.

Park, S., Lee, Y., Lee, J.H., and Jin, E. (2013). Expression of the high light-inducible *Dunaliella LIP* promoter in *Chlamydomonas reinhardtii*. Planta **238**:1147–1156.

Pérez-Pérez, M.E., Zaffagnini, M., Marchand, C.H., Crespo, J.L., and Lemaire, S.D. (2014). The yeast autophagy protease Atg4 is regulated by thioredoxin. Autophagy **10**:1953–1964.

Pfaffl, M.W. (2001). A new mathematical model for relative quantification in real-time RT-PCR. Nucleic Acids Res. **29**:e45.

Piechota, J., Kolodziejczak, M., Juszczak, I., Sakamoto, W., and Janska, H. (2010). Identification and characterization of high molecular weight complexes formed by matrix AAA proteases and prohibitins in mitochondria of *Arabidopsis thaliana*. J. Biol. Chem. **285**:12512–12521.

Pribil, M., Labs, M., and Leister, D. (2014). Structure and dynamics of thylakoids in land plants. J. Exp. Bot. **65**:1955–1972.

Puthiyaveetil, S., Tsabari, O., Lowry, T., Lenhert, S., Lewis, R.R., Reich, Z., and Kirchhoff, H. (2014). Compartmentalization of the protein repair machinery in photosynthetic membranes. Proc. Natl. Acad. Sci. USA **111**:15839–15844.

Qi, Y., Liu, X., Liang, S., Wang, R., Li, Y., Zhao, J., Shao, J., An, L., and Yu, F. (2016). A putative chloroplast thylakoid metalloprotease VIRESCENT3 regulates chloroplast development in *Arabidopsis thaliana*. J. Biol. Chem. **291**:3319–3332.

Rappaport, F., Béal, D., Joliot, A., and Joliot, P. (2007). On the advantages of using green light to study fluorescence yield changes in leaves. Biochim. Biophys. Acta **1767**:56–65.

Risør, M.W., Poulsen, E.T., Toftgaard Thomsen, L.R., Dyrlund, T.F., Nielsen, T.A., Nielsen, N.C., Sanggaard, K.W., and Enghild, J.J. (2014). The autolysis of human HtrA1 is governed by the redox states of its N-terminal domain. Biochemistry **53**:3851–3857.

Rodrigues, R.A., Silva-Filho, M.C., and Cline, K. (2011). FtsH2 and FtsH5: two homologous subunits use different integration mechanisms leading to the same thylakoid multimeric complex. Plant J. **65**:600–609.

Rymarquis, L.A., Handley, J.M., Thomas, M., and Stern, D.B. (2005). Beyond complementation. Map-based cloning in *Chlamydomonas reinhardtii*. Plant Physiol. **137**:557–566.

Sacharz, J., Bryan, S.J., Yu, J., Burroughs, N.J., Spence, E.M., Nixon, P.J., and Mullineaux, C.W. (2015). Sub-cellular location of FtsH proteases in the cyanobacterium Synechocystis sp. PCC 6803 suggests localised PSII repair zones in the thylakoid membranes. Mol. Microbiol. **96**:448–462.

Sakamoto, W., Tamura, T., Hanba-Tomita, Y., Murata, M., Sodmergen, and Murata, M. (2002). The *VAR1* locus of *Arabidopsis* encodes a chloroplastic FtsH and is responsible for leaf variegation in the mutant alleles. Genes Cells **7**:769–780.

Saikawa, N., Akiyama, Y., and Ito, K. (2004). FtsH exists as an exceptionally large complex containing HflKC in the plasma membrane of *Escherichia coli*. J. Struct. Biol. **146**:123–129.

Saint-Marcoux, D., Wollman, F.A., and de Vitry, C. (2009). Biogenesis of cytochrome b_6 in photosynthetic membranes. J. Cell. Biol. **185**:1195–1207.

Sambrook, J., and Russell, D.W. (2001). Molecular Cloning: A Laboratory Manual, 3rd edn (New York: Cold Spring Harbor Laboratory Press).

Schloss, J.A. (1990). A *Chlamydomonas* gene encodes a G protein beta subunit-like polypeptide. Mol. Gen. Genet. **221**:443–452.

Schmidt, T.G.M., and Skerra, A. (2007). The *Strep*-tag system for one-step purification and high-affinity detection or capturing of proteins. Nat. Protoc. **2**:1528–1535.

Shimogawara, K., Fujiwara, S., Grossman, A., and Usuda, H. (1998). High efficiency transformation of *Chlamydomonas reinhardtii* by electroporation. Genetics **148**:1821–1828.

Sinvany-Villalobo, G., Davydov, O., Ben-Ari, G., Zaltsman, A., Raskind, A., and Adam, Z. (2004). Expression in multigene families. Analysis of chloroplast and mitochondrial proteases. Plant Physiol. **135**:1336–1345.

Ströher, E., and Dietz, K.J. (2008). The dynamic thiol-disulphide redox proteome of the *Arabidopsis thaliana* chloroplast as revealed by differential electrophoretic mobility. Physiol. Plant. **133**:566–583.

Steglich, G., Neupert, W., and Langer, T. (1999). Prohibitins regulate membrane protein degradation by the m-AAA protease in mitochondria. Mol. Cell. Biol. **19**:3435–3442.

Sun, X., Peng, L., Guo, J., Chi, W., Ma, J., Lu, C., and Zhang, L. (2007). Formation of DEG5 and DEG8 complexes and their involvement in the degradation of photodamaged photosystem II reaction center D1 protein in *Arabidopsis*. Plant Cell **19**:1347–1361.

Szilárd, A., Sass, L., Hideg, E., and Vass, I. (2005). Photoinactivation of photosystem II by flashing light. Photosynth. Res. **84**:15–20.

Szyszka-Mroz, B., Pittock, P., Ivanov, A.G., Lajoie, G., and Hüner, N.P. (2015). The Antarctic psychrophile, *Chlamydomonas* sp. UWO 241, preferentially phosphorylates a PSI-cytochrome b_6/f supercomplex. Plant Physiol. **169**:717–736.

Thomas, P.E., Ryan, D., and Levin, W. (1976). An improved staining procedure for the detection of the peroxidase activity of cytochrome P-450 on sodium dodecyl sulfate polyacrylamide gels. Anal. Biochem. **75**:168–176.

Trösch, R., Mühlhaus, T., Schroda, M., and Willmund, F. (2015). ATP-dependent molecular chaperones in plastids—more complex than expected. Biochim. Biophys. Acta **1847**:872–888.

Wang, H., Gau, B., Slade, W.O., Juergens, M., Li, P., and Hicks, L.M. (2014). The global phosphoproteome of *Chlamydomonas reinhardtii* reveals complex organellar phosphorylation in the flagella and thylakoid membrane. Mol. Cell. Proteomics **13**:2337–2353.

Wei, L., Derrien, B., Gautier, A., Houille-Vernes, L., Boulouis, A., Saint-Marcoux, D., Malnoë, A., Rappaport, F., de Vitry, C., Vallon, O., et al. (2014). Nitric oxide-triggered remodeling of chloroplast bioenergetics and thylakoid proteins upon nitrogen starvation in *Chlamydomonas reinhardtii*. Plant Cell **26**:353–372.

Yoshioka, M., Nakayama, Y., Yoshida, M., Ohashi, K., Morita, N., Kobayashi, H., and Yamamoto, Y. (2010). Quality control of photosystem II: FtsH hexamers are localized near photosystem II at grana for the swift repair of damage. J. Biol. Chem. **285**:41972–41981.

Yoshioka, M., and Yamamoto, Y. (2011). Quality control of Photosystem II: where and how does the degradation start under light stress?—Facts and hypotheses. J. Photochem. Photobiol. B **104**:229–235.

Yoshioka-Nishimura, M., Nanba, D., Takaki, T., Ohba, C., Tsumura, N., Morita, N., Sakamoto, H., Murata, K., and Yamamoto, Y. (2015). Quality control of photosystem II: direct imaging of the changes in the thylakoid structure and distribution of FtsH proteases in spinach chloroplasts under light stress. Plant Cell Physiol. **55**:1255–1265.

Yu, F., Park, S., and Rodermel, S.R. (2004). The *Arabidopsis* FtsH metalloprotease gene family: interchangeability of subunits in chloroplast oligomeric complexes. Plant J. **37**:864–876.

Yu, F., Park, S., and Rodermel, S.R. (2005). Functional redundancy of AtFtsH metalloproteases in thylakoid membrane complexes. Plant Physiol. **138**:1957–1966.

Zaltsman, A., Feder, A., and Adam, Z. (2005a). Developmental and light effects on the accumulation of FtsH protease in *Arabidopsis* chloroplasts-implications for thylakoid formation and photosystem II maintenance. Plant J. **42**:609–617.

Zaltsman, A., Ori, N., and Adam, Z. (2005b). Two types of FtsH protease subunits are required for chloroplast biogenesis and Photosystem II repair in *Arabidopsis*. Plant Cell **17**:2782–2790.

Zhang, D., Kato, Y., Zhang, L., Fujimoto, M., Tsutsumi, N., Sodmergen, and Sakamoto, W. (2010). The FtsH protease heterocomplex in *Arabidopsis*: dispensability of type-B protease activity for proper chloroplast development. Plant Cell **22**:3710–3725.

Zhang, L., Wei, Q., Wu, W., Cheng, Y., Hu, G., Hu, F., Sun, Y., Zhu, Y., Sakamoto, W., and Huang, J. (2009). Activation of the heterotrimeric G protein alpha-subunit GPA1 suppresses the ftsh-mediated inhibition of chloroplast development in *Arabidopsis*. Plant J. **58**:1041–1053.